Toward a Systematic Framework for Deploying Synchrophasors and their Utilization for Improving Performance of Future Electric Energy Systems

Final Project Report

Power Systems Engineering Research Center

Empowering Minds to Engineer
the Future Electric Energy System

Toward a Systematic Framework for Deploying Synchrophasors and their Utilization for Improving Performance of Future Electric Energy Systems

Part A, B and C

Final Project Report

Part A Project Team
Marija Ilic, Project Leader
Qixing Liu, Graduate Student
Carnegie Mellon University

Part B Project Team
Vaithianathan "Mani" Venkaatsubramanian, Project Leader
Xing Liu, Javier Guerrero, Hong Chun, Graduate Students
Washington State University

Part C Project Team
Ali Abur, Project Leader
Roozbeh Emami, Graduate Student
Northeastern University

PSERC Publication 12-18

May 2012

Information about this project

For information about this project contact:

Marija Ilic
Professor, School of Electrical an Computer Engineering
Carnegie Mellon University, Pittsburgh, PA 15213
Tel: 412-268-9520
Fax: 412-268-3890
Email: milic@ece.cmu.edu

Power Systems Engineering Research Center

The Power Systems Engineering Research Center (PSERC) is a multi-university Center conducting research on challenges facing the electric power industry and educating the next generation of power engineers. More information about PSERC can be found at the Center's website: http://www.pserc.org.

For additional information, contact:

Power Systems Engineering Research Center
Arizona State University
527 Engineering Research Center
Tempe, Arizona 85287-5706
Phone: 480-965-1643
Fax: 480-965-0745

Notice Concerning Copyright Material

Acknowledgements

This is the final report for the Power Systems Engineering Research Center (PSERC) research project titled "Toward a Systematic Framework for Deploying Synchrophasors and their Utilization for Improving Performance of Future Electric Energy Systems." We express our appreciation for the support provided by PSERC's industrial members.

We wish to thank all our industry advisors Lisa Beard (TVA- now Quanta Technology), Floyd Galvan (Entergy), Jim Gronquist (BPA), Paul Myrda (EPRI), Antony Johnson (SCE), Mahendra Patel (PJM), Innocent Kamwa (Hydro-Quebec/IREQ), Kip Morison (BCTC- now BC Hydro), Navin Bhatt (AEP), and Reynaldo Nuqui (ABB). Moreover, the project leader of Part B wishes to thank James Ritchie Carroll at Tennessee Valley Authority (TVA) (now at Grid Protection Alliance) for helping the project team with the prototype implementation testing of the PMU based voltage stability monitor at TVA, also, Farrokh "Frank" Habibi-Ashrafi and Armando Salazar at Southern California Edison (SCE) for collaborating with the WSU project team on subsequent research and prototype implementation work of PMU based substation voltage controller for SCE power system. The project leader of Part C wishes to thank Dr. Jianzhong Tong of PJM and Dr. Jay Giri of Alstom Grid.

Executive Summary

This report is motivated by the major opportunities offered by the deployment of near-real time synchrophasor measurements. For the first time it has become possible to consider wide-area synchronized sensing, communications and use for automated control and protection. These opportunities are presenting the industry and the research community with many open questions, not all of which can be addressed in a single report. In this sense the report provides samples of possible uses of synchrophasors for estimation and control. The ultimate objective is to utilize synchrophasors for improving performance of future electric energy systems.

Part A of this report shows how synchrophasor measurements can be used to close the loop and regulate key, pilot point, voltages in each control area and/or regulate the deviations in tie-line flow exchanges between the control areas. The major contribution is a systematic method for selecting the most effective locations for monitoring voltage deviations to be used for closing the loop and for adjusting set points of generators participating in this regulation. It is stressed that while this control scheme has been in place for a very long time in France, the optimal selection of pilot points has remained an open theoretical problem. In this report we introduce a systematic method for selecting the most effective locations for placing synchrophasors to be managing effects of slow voltage deviations around the forecast reactive power demand.

Part A specifically concerns new design of Automated Voltage Regulation (AVR) and Automated Flow Regulation (AFR), which relies on the use of synchrophasors. This control is also known as the Secondary Voltage Control (SVC) and Pennsylvania Jersey Maryland (PJM) currently uses it by the Electricite de France, and, more recently. Its basic purpose is to regulate in an automated way voltage deviations around their schedules that are caused by the relatively slow voltage deviations. The best way of thinking about it is as the sister-function to the Automatic Generation Control (AGC). Instead of regulating single frequency in each control area, it is intended to regulate several voltages to their scheduled values by adjusting the set points of Automatic Voltage Regulators (AVRs) on several generators participating in this scheme. This scheme is necessary to manage the effects of the increased presence of quasi-stationary disturbances causing deviations in voltages around the values resulting from regular 15-30 minute generation dispatch. In particular, these disturbances are caused by persistent hard-to-predict wind power deviations and by the increasingly responsive demand to real-time electricity prices.

Assuming the dynamics resulted from these disturbances could be stabilized by primary control, reliability problems will still remain in forms of system-wide load voltage deviations and transmission line power flow deviations around their scheduled values. It is, therefore, important to maintain load voltages and transmission line power flows within the pre-specified limits as disturbances around scheduled real/reactive power generation dispatch take place.

The implementation of AVR/SVC for purposes of regulating voltage and flow deviations can be done using measurements provided by the Phasor Measurement Units (PMUs). PMUs could provide accurate and fast sensing of key output variables of interest. We pose the problem of PMU-enabled AVC and AFC as an engineering design problem which for the given number of PMUs computes the best locations of PMUs and the control design gains based on these measurements in order to ensure that the voltage and/or flow deviations remain within the pre-specified limits. We describe in this report how to pose systematically the problems of robust Automated Voltage Control (AVC) and Automated Flow Control (AFC) design based on selecting the best locations for placing the PMUs and the corresponding feedback control gains. The underlying mathematical formulation is the minimization of L_∞ norm representing the measure of the worst-case deviations. Once the problem is posed, a Linear Programming (LP) algorithm is used to find numerical solutions which minimize this objective function; simulations are carried out to show the result of using the LP method. In the latter part of this report, a design of decentralized AVC for very large-scale power systems has also been formulated. This is based on a multi-layered clustering algorithm for decomposing the system into several weakly interconnected reactive power control zones. These zones can be computed once and/or can be dynamically recomputed operating conditions vary. For dynamically clustered approach generally a higher number of PMUs is required. The results are illustrated by simulating potential performance of the proposed designs using an equivalent Northeast Power Coordinating Council 36-bus system. The results indicate that the *N-1* reliability criteria can be met by combining the economic dispatch for scheduling resources given demand forecast, and by relying on an automated feedback to ensure that voltage and line flow deviations remain within the pre-specified limits in between scheduling intervals. This is done without having to know the exact location and magnitude of disturbances.

Part B of this report proposes a synchrophasors-based substation voltage controller. Novel algorithms for direct estimation of QV line sensitivities from real-time streaming PMU data are proposed first. The algorithms are shown to be effective in detecting voltage insecurity scenarios in the power system. Voltage Security Index proposed at each bus is useful to classify voltage strong buses versus voltage weak buses in terms of reactive power support at the bus. Next, initial formulation of a substation voltage controller is proposed. The controller uses QV sensitivity values from Section 2 to carry out local power-flow like calculations to predict expected bus voltage levels after discrete switching actions. The substation controller then coordinates the switching of local VAR devices to manage the discrete VAR devices at the substation towards maintaining voltage schedules for different voltage levels at the substation. Future research is indicated on two-level control formulations that may include central higher-level coordinator and many local substation controllers.

Finally, Part C of this report is concerned with a development of a practical method to identify the external line outages using the data available to internal power system operator in real-time, namely real-time data from internal system as well as measurements from those external buses with PMUs. In an inter-connected power system, state estimator has real-time access to the measurements, and topology of the area under

study, while its real-time knowledge about external system measurements and topology is very limited. One way to have real-time access to external measurements and topology is through phasor measurement units (PMUs).

Errors in external network topology may have significant impact on accuracy of internal state estimation and subsequent real-time contingency analysis (especially contingency analysis). Identification of any type of change in the external network topology will be impossible by using only internal system real-time measurements. However, recent availability of external system synchronized phasor measurements will facilitate identification of certain external topology errors, especially if they are strategically located with respect to the available phasor measurement units. The proposed method is developed and presented in two parts: In the first part the problem of external topology change is formulated using DC power flow assumptions. Once the formulated problem is solved successfully, the method can be extended to the more realistic AC power flow formulation. In the second part, the developed method is extended to the non-linear case of full A.C. solution. In addition to the internal system measurements, few phasor measurements installed in the external system are also assumed to exist in this part. The proposed method utilizes an integer programming method to identify the changes in external system based on real-time data received from internal system along with real-time data from external phasor measurement units. The linear (D.C.) decoupled model of the power system will be used initially to formulate the external network topology-tracking problem and develop its solution method.

It has been important for the proposed method to address all possible conditions in the external system. The proposed method is required to accurately detect an external load change as an external topology change and vice versa. Different possible scenarios which the proposed method would be able to identify can be listed as follows: a) External topology change with constant external operating conditions; b) External operating change with constant external topology; c) Change in neither external topology nor external operating conditions; and, d) Change in both external system operating conditions and external network topology.

The proposed method utilizes an integer programming method to identify the changes in external system based on real-time data received from internal system along with real-time data from external phasor measurement units. The linear (D.C.) decoupled model of the power system will be used initially to formulate the external network topology tracking problem and develop its solution method.

The proposed method's performance is tested using the IEEE 30 bus and 118 bus test systems.

Towards Electric Power System Automated Voltage and Flow Regulation with Phasor Measurement Units

Part A

Part A Project Team

Marija Ilic, Project Leader
Qixing Liu, Graduate Student
Carnegie Mellon University

Information about Part A

For information about Part A of this report contact:

Marija Ilic
Professor, School of Electrical an Computer Engineering
Carnegie Mellon University, Pittsburgh, PA 15213
Tel: 412-268-9520
Fax: 412-268-3890
Email: milic@ece.cmu.edu

Power Systems Engineering Research Center

The Power Systems Engineering Research Center (PSERC) is a multi-university Center conducting research on challenges facing the electric power industry and educating the next generation of power engineers. More information about PSERC can be found at the Center's website: http://www.pserc.org.

For additional information, contact:

Power Systems Engineering Research Center
Arizona State University
527 Engineering Research Center
Tempe, Arizona 85287-5706
Phone: 480-965-1643
Fax: 480-965-0745

Notice Concerning Copyright Material

PSERC members are given permission to copy without fee all or part of this publication for internal use if appropriate attribution is given to this document as the source material. This report is available for downloading from the PSERC website.

Contents

1 Part A Summary: Toward PMU Enabled AVC and AFC 1

2 Introduction 3

2.1 Motivation 3

2.2 Literature Review 5

2.3 Approach Proposed in This Report 6

2.4 Preview of Chapters 7

3 PMU-based Automated Voltage Control Design 8

3.1 Modeling of Automated Voltage Control Problem 8

3.2 Illustration of the AVC Design on a Small 5-bus Electric Power System 12

3.3 Transferring Control Objective Function to Linear Programming Problem . . 13

4 PMU-based Automated Flow Control Design 14

4.1 Illustration of the AFC Design on a Small 5-bus Electric Power System 17

4.2 Transferring Control Objective Function to Linear Programming Problem . . 18

5 A Multi-Layered Clustering Algorithm for Determining Secondary Control Zones . . 19

5.1 Numerical Problems With A Single-Layer Clustering Algorithm 20

5.2 A Novel Numerically Stable Multi-Layered Clustering Algorithm 21

6 Communication Architecture for the Implementation of PMU-based Secondary Controls 22

6.1 Introduction to Phasor Measurement Units 22

6.2 Communication Architecture for Secondary Level Control in Different-Amount-of-Information Cases 25

7 Experimental Simulation Studies 26

7.1 Simulation Studies of Robust AVC on NPCC Power System 31

7.2 Simulation Studies of Robust AFC on NPCC Power System 32

8 Conclusions 38
8.1 Contributions of This Report 38
8.2 Future Work 39

List of Figures

1 PMU-based AVC on 5-bus Power System 13
2 PMU-based AFC on 5-bus Power System 18
3 The First PMU Developed in Virginia Tech in 1980s [1] 24
4 Illustration of Sinusoid Wave and Its Phasor Representation 24
5 Estimation of Phasors from Sampled Data Using Discrete Fourier Transform [1] . . . 25
6 Communication Architecture of Conventional ACE-based AGC 27
7 Communication Architecture of AVC with Limited Information 28
8 Communication Architecture of AVC with Full Information 28
9 Communication Architecture of AFC with Limited Information 29
10 Communication Architecture of AFC with Full Information 29
11 One Line Diagram of the Equovalenced NPCC 36-bus Power System 30
12 Robust AVC Applied to NPCC in both Limited and Full Information Cases 33
13 The Multi-layered Clustering Algorithm Applied to NPCC Power System 34
14 Robust AVC Applied to NPCC after Clustering 35
15 Robust AFC Applied to NPCC in both Limited and Full Information Cases 37

List of Tables

1 Bus-types of the Tested NPCC Power System 27
2 Pilot-points Locations and Optimal Control Gains for the Robust AVC in NPCC System 31
3 Pilot-points Locations and Optimal Control Gains for the Robust AFC in NPCC System 36

1 Part A Summary: Toward PMU Enabled AVC and AFC

This is a research report on Part A of this project. It specifically concerns new design of Automated Voltage Regulation (AVR) and Automated Flow Regulation (AFR) which relies on the use of PMUs. In order to avoid confusion in relation to the already established term for Automatic Voltage Control (AVC) we use the same term. Namely, this is not automated primary control of AVRs. The AVC term as currently used by the Electricite de France, and, more recently by PJM, is effectively an AVR scheme. Its basic purpose is to regulate in an automated way voltage deviations around their schedules that are caused by the relatively slow voltage deviations. The best way of thinking about it is as the sister-function to the Automatic Generation Control (AGC). Instead of regulating single frequency in each control area, it is intended to regulate several voltages to their scheduled values by adjusting the set points of Automatic Voltage Regulators (AVRs) on several generators participating in this scheme. This scheme is necessary to manage the effects of the increased presence of quasi-stationary disturbances causing deviations in voltages around the values resulting from regular 15-30 minute generation dispatch. In particular, these disturbances are caused by persistent hard-to-predict wind power deviations and by the increasingly responsive demand to real time electricity prices.

Assuming the dynamics resulted from these disturbances could be stabilized by primary control, reliability problems will still remain in forms of system-wide load voltage deviations and transmission line power flow deviations around their scheduled values. It is, therefore, important to maintain load voltages and transmission line power flows within the pre-specified limits as disturbances around scheduled real/reactive power generation dispatch take place.

The implementation of AVC for purposes of regulating voltage and flow deviations can be done using measurements provided by the Phasor Measurement Units (PMUs). PMUs could provide accurate and fast sensing of key output variables of interest. We pose the problem of PMU-enabled AVC and AFC as an engineering design problem which for the given number of PMUs computes the best locations of PMUs and the control design gains based on these measurements in order to ensure that the voltage and/or flow deviations remain within the pre-specified limits. we describe in this report how to pose systematically the problems of robust Automated Voltage Control (AVC) and Automated Flow Control (AFC) design based on selecting the best locations for placing the PMUs and the corresponding feedback control gains. The underlying mathematical formulation is the

minimization of L_∞ norm representing the measure of he worst-case deviations. Once the problem is posed, a Linear Programming (LP) algorithm is used to find numerical solutions which minimize this objective function; simulations are carried our to show the result of using the LP method. In the latter part of this report, a design of decentralized AVC for very large-scale power systems has also been formulated, This is based on a multi-layered clustering algorithm for decomposing the system into several weakly interconnected reactive power control zones. These zones can be computed once and/or can be dynamically recomputed a operating conditions vary. For dynamically clustered approach generally a higher number of PMUs is required. The results are illustrated by simulating potential performance of the proposed designs using an equivalent Northeast Power Coordinating Council 36-bus system. The results indicate that the $(N-1)$ reliability criteria can be met by combining the economic dispatch for scheduling resources given demand forecast, and by relying on an automated feedback to ensure that voltage and line flow deviations remain within the pre-specified limits in between scheduling intervals. This is done without having to know the exact location and magnitude of disturbances.

2 Introduction

2.1 Motivation

The control of voltage and reactive power has been long recognized as an important problem in power system operation. Due to economic and environmental considerations, power systems are operated closer to their voltage stability limits; so it becomes difficult to control the reactive power demand of those systems. The lack of reactive power support may affect the systems voltage stability and lead to voltage collapse incident [2, 3]. The first motivation of this report is to design an secondary automated voltage control (AVC) based on Phasor Measurement Units (PMUs) to regulate the voltage deviations in load buses caused by load demand fluctuations from normal operating conditions over a variety of time scales. It is consistent with the conventionally proposed hierarchical structure which is an aggregation of primary, secondary and tertiary control [4, 5, 6, 7].

In the hierarchically based modeling and control approach, a large-scale interconnected power system is first decomposed into administratively separate regions. Each region has independent controls and makes its own decisions. Primary voltage control is provided by reactive power compensation facilities or automatic voltage regulators (AVR) on individual synchronous generating units of each region. It mainly responds to the local disturbances and acts to maintain the local outputs close to the values of quasi steady state set points. The task of secondary voltage control is to adjust the reference values for reactive power primary controls in a coordinated way in case that the system experiences unusual reactive power deficiency because of large disturbance from the fluctuations in load and renewable generation or tripping of generating units. It is keeping the purpose in mind that the region-wide voltage deviations should be limited within some reliability criteria. Tertiary control is the coordination of the regional secondary controls to satisfy system-wide operating criteria, such as economic and secure operation of the whole electric network. Currently, electric power systems in Spain, France and Italy are the systems which have critical implementation of this structurally based voltage control with automatic adjustment in the secondary level [5, 8, 9, 10].

The existing close-loop secondary voltage control schemes mainly utilizes the information of a few key buses called pilot-points as feedback. Traditionally, feedback information is provided by SCADA/EMS (Supervisory Control And Data Acquisition and Energy Management System) which refreshes the system steady states in every 2-10 seconds. It takes so much time since all SCADA

data must be sent to a central location and the centralized state estimator consumes a long time on data processing and state estimation to provide system operator with system states as accurate as it could through EMS. This will not cause a problem before the system restructuring and renewable generation integration start to introduce disturbance with higher frequency and magnitude than it was. Today's SCADA/EMS is highly possible to fail to capture the system states just in time. For example, in the case that secondary voltage control is supposed to operate in every ONE second to adjust the set-points of AVRs, the conventional SCADA/EMS will not be able to cope with this commission at all! For this reason, the implementation of PMUs becomes necessary for next generation's automated voltage control. Phasor measurement technology [11, 12, 1, 13] is recently developed which receives signals from Global Positioning System (GPS) satellites as a kind of time reference from radio clock. The sampling clocks of PMUs are then synchronized with the radio time reference so that the measurement of voltage and current phasors will be time-stamped in a systematic point of view. Because these phasors are truely synchronized, comparison and the control of the system states quantities in real time is possible. Plus the direct measurement of system states, PMUs measure much faster and more accurate than other commonly used meters and devices; and the fire-optical based communication network connecting these sensors transmits data much faster than the cable based communication network. Such features guarantee that PMUs can satisfy the requirement of the improved secondary voltage control in modern power systems by providing the information just in time and just in context.

In a parallel way to the PMU-based AVC, the problem of designing PMU-based automate flow control (AFC) is formulated, which is the second motivation of this report. This is a new concept. Basically, AFC is also a secondary level control which adjusts the set-points of real power primary controls coordinately in order to ensure that the real power transmission in significant tie-lines are limited as close as possible to their pre-specified values. This is important because currently power systems are being operated near their transmitting capacities and some transmission lines are heavy loaded and undergoing congestions due to the constraints that every physical line in power grid has its own thermal limit and the more it transmits power, the closer it is towards the thermal limit. However, it is even worse when the power system stability problem is taken into consideration, which allows the transmission lines to transmit much lower than its thermal limit. Large deviation of real power flows in a heavy loaded transmission line may therefore violate its transmitting limit

and cause the protective relays to trip off the line from system operation. It actually changes the system topology and is possible to introduce more sequent troubles to the system than expectation. One problem is defined in many literatures as cascading failures and also observed in the 2003 U.S.-Canada blackout [2, 14]. When the heavy loaded transmission line gets tripped from system operation, its load will be transferred to other transmission lines nearby. If unfortunately these lines are heavy loaded as well, the sudden power increase will push these line towards or even violate their transmitting limits. Consequently, more and more transmission lines will get tripped and the system loses a large amount of its transmitting capability, which is just the point for blackout to happen. On the other hand, the deviation in inter-area tie-line flow from the pre-scheduled value will cause frequency problems in the control areas connected by this tie-line. This problem is partly covered by today's Automated Generation Control (AGC) but in a way that is not so sophisticated. AFC is proposed to prevent these kind of events from happening by restricting the tie-line flow deviation within the reliability criteria. In the scheme proposed in this report, the role of PMUs is the key since it is not possible to implement AFC without measuring the voltage phase angles of the pilot-points in a fast and accurate manner.

2.2 Literature Review

An overview of the extensive literatures indicates that in secondary voltage control, the mean of selecting pilot-points and the designing automated control law given the information from pilot buses have been paid much attention. In [8, 9], electrical distance matrix built on the sensitivity matrix of variation in voltage with respect to injection of reactive power is used to study the structure of French EHV power system. It divides the power system into uncoupled control zones by ascending hierarchical classification and the method of dynamic scatter. Best number of control zones is found by coordinating the group number and grouping distances. Then, the bus which locates in the electrical distance center of each zone is adopted as the pilot point.

Ref [5] presents the progress of Spanish researchers. In their point of view, secondary voltage control selects the pilot buses by solving a nonlinear integer optimization problem off-line. Greedy algorithm and Global search method are employed to find the optimal number and positions of pilot-points. An optimal control scheme is then proposed based on the information from pilot-points. In every control step, it is designed to keep voltage magnitude of these pilot buses in their respective

reference values, and on the other hand to achieve a similar relative reactive power loading of the control generators. However, there is no clustering in this approach to decompose the power system into different weakly coupled control zones. Instead, power flow equations are solved by considering the system as a whole after every control step to update the phasor information of bus voltages. This may become the bottleneck of the application of this approach to fast automated voltage control in large-scale power systems. The reason is that solving both the optimal control objective function and the later power flow equations in a centralized way requires much computation efforts for large power systems. So fast AVC which is in second level turns to be very hard to achieve.

2.3 Approach Proposed in This Report

In this report, for power system under a class of disturbances, robust AVC and AFC are proposed to minimize the worst voltage deviation on load buses and flow deviation on transmission lines. Both reactive power and real power disturbances from the loads are assumed to stay within a boundary, $|\Delta Q_L|_\infty \leq \gamma$ and $|\Delta P_L|_\infty \leq \rho$. The work is based on previous studies on optimal secondary voltage control [15] which addressed the problems of pilot-points selection and secondary voltage control by solving a group of L_∞ norm minimization objective functions. It employs the linear feedback scheme to design the pilot-point information based control. L_∞ norm minimization is used here in order to keep the worst-case load voltage deviation within pre-specified limits as long as the disturbance remain within its boundary. The output gives the optimal control gain for each reactive power control source to adjust its reactive power set-point corresponding to the change in pilot-points voltage magnitude. One variable inside of this function is about the pilot-points. The number and positions of pilot-points must be pre-set when the L_∞ norm minimization is ready to be solved. The approach then selects the best locations of pilot-points through an extensive search over all possible combinations of the pilot buses in the situation that the number of pilot-points is given. In other words, the output feedback control gains of the L_∞ norm optimization problems are compared by giving the same number but spatially different combinations of pilot-points. The best locations then emerge out of the comparison.

In the work of this report, besides formulating the new concept AFC and the conventional AVC both to L_∞ norm optimization problems the same as [15], a technique to solve the problems in an effective way is also developed. The original objective function that minimizes the L_∞ norm

is equivalently transferred to a Linear Programming (LP) program; and by solving the new LP problem, we will be able to get the optimal control gain for each reactive power and real power control source. However, as the system complexity grows along with the increasing in its size, even solving LP problem consumes much time on computation. In this case, a clustering method based on the normalized electrical distance matrix [16] is introduced to divide the large-scale power system into proper number of control zones. The optimization problems of AVC and AFC design are then adopted to each control zone to select the best locations of pilot-points and the relevant optimal control gains of its own. Moreover, instead of obtaining the information from SCADA/EMS, PMUs are installed to the selected pilot-points as fast measurement to close the feedback control loop. In AVC, voltage magnitudes are measured from the pilot buses; while in AFC, voltage phase angles are measured. In general, work of this report provides the opportunity to automatically adjust the set-points of both reactive power and real power controllers in a secondary control level close to every 1 second.

2.4 Preview of Chapters

In this report, Chapter 1 gives the general introduction of the motivation of our work, the existing methods to deal with the similar problem as well as the approach proposed in our work. Chapters 2 and 3 pose the problem and solution of robust AVC and AFC respectively. Chapter 4 introduces the clustering method that is used to decompose large power systems. Chapter 5 demonstrates the simulation results based on a commonly used power system model to support the approach. Chapter 6 makes the conclusion for this report.

Chapter 2 starts from formulating the robust AVC into the L_∞ norm optimization problem. Linear feedback control scheme is adopted to design the optimal control that adjusts the set-point of reactive control sources with respect to the voltage magnitude change on pilot buses. Then the reformulation of this optimization problem into Linear Programming problem is stated.

Chapter 3 illustrates the formulation of robust AFC similar to Chapter 2. The problem is transferred to LP problem afterwards.

In Chapter 4, a clustering algorithm based on the normalized electrical distance matrix is introduced to create weakly coupled control zones inside of the system. To overcome the problem that the single-layer clustering method originated from Ref [16] sometimes fails to give the resulting zones

of nearly equal size and not excessively large, a novel numerically stable multi-layered clustering algorithm is then proposed as an enhancement.

In Chapter 5, a communication architecture is proposed to comprise the measurement from both PMUs and conventional SCADA system and the communication channels that transmit the monitoring information of bus voltage and phase angle to the control center and distribute the control signal to generators or other control resources from the control center. Features of PMUs and the sampling and communication issues are also introduced to support the feasibility of the robust AVC and AFC on measurement and communication side.

In Chapter 6, simulations are carried out on the 36-Bus Northeast Power Coordinating Council (NPCC) equivalent power system model. Different cases like 1 pilot-point, 2 pilot-points and all load buses monitored (PMU in every load bus) with and without clustering the system into control zones are studied respectively. By taking the simulation results as consideration, the approaches illustrated in previous chapters are verified.

Chapter 7 concludes the contributions of this report and suggests possible future work.

3 PMU-based Automated Voltage Control Design

3.1 Modeling of Automated Voltage Control Problem

In this chapter, the problem of robust Automated Voltage Control (AVC) is precisely defined. Optimal number of pilot points is found through the exhaustive comparison among worst cases studies when each case is with a different number of pilot points but the same control design algorithm is taken into implementation. Studies on worst case performance is the appropriate point of investigation to this robust AVC problem because every load bus voltage must be held within tolerable limit.

The basic problem is formulated as in [15]. The secondary voltage control is intended to regulate voltage deviations in response to relatively small disturbances in reactive power, and consequently, the deviation of closed-loop load voltages are expected not to to vary significantly around the scheduled (nominal) voltages. This makes it possible to use a linearized model. Small reactive power load disturbances ΔQ_L are causing deviations in load voltages and the PMUs are used to measure the zonal pilot points load voltage deviations ΔV_p. Control gains are computed so

that the closed-loop load voltage deviations are minimized for any disturbance. If, in addition, the disturbance bounds are given, the gains and measurement locations are computed so the load deviations remain robust with respect to disturbances. Namely, an off-line design is carried out to ensure that load voltage deviations remain within the pre-specified limits. The minimization of L_∞ (the largest) norm control design can ensure that the system worst voltage deviation remains within the given limits.

To re-formulate this worst case robust optimization problem as introduced some time ago in [15], we start by stating the decoupled linearized reactive power-voltage constraints subject to which the optimization is done. These are obtained by simply using decoupled reactive power-voltage $Q - V$ Jacobian computed at the given nominal operating point.

$$\begin{bmatrix} \Delta Q_G \\ \Delta Q_L \end{bmatrix} = \begin{bmatrix} B_{GG} & B_{GL} \\ B_{LG} & B_{LL} \end{bmatrix} \begin{bmatrix} \Delta V_G \\ \Delta V_L \end{bmatrix} \tag{1}$$

In equation (1), ΔQ_G and ΔV_G are the reactive power and voltage increment of generator buses (subscript G stands for generator); ΔQ_L and ΔV_L are the reactive power and voltage increment of load buses (subscript L stands for load). We next rewrite Equation (1) by inverting the B matrix.

$$\begin{bmatrix} \Delta V_G \\ \Delta V_L \end{bmatrix} = \begin{bmatrix} Z_{GG} & Z_{GL} \\ Z_{LG} & Z_{LL} \end{bmatrix} \begin{bmatrix} \Delta Q_G \\ \Delta Q_L \end{bmatrix} \tag{2}$$

where $Z = B^{-1}$. In this equation, the voltage deviations on generator buses are assumed to be compensated by the primary controls in a much smaller time scale than the adjustment of reactive power set-points in secondary level. In other words, there is no need for secondary control to recover or limit the voltage deviations of generator buses because these the primary controls such as Automated Voltage Regulators (AVRs) or shunt capacitors have already acted to keep the voltage of generators at the set-points to make $\Delta V_G \equiv 0$. Only load-bus voltages will be impacted by change in reactive power consumption from load buses and production from generator buses, which is derived from equation (2):

$$\Delta V_L = Z_{LL}\Delta Q_L + Z_{LG}\Delta Q_G \tag{3}$$

In this equation, ΔQ_G is the term that is controllable by AVRs or shunt capacitors; while ΔQ_L is considered to be the source of disturbance for secondary control because it is naturally varying around the nominal operating point and uncontrollable for system operators. As a result, the

philosophy of secondary voltage control can be interpreted as regulating the system-wide load-bus voltage deviations caused by load-bus reactive power disturbances ΔQ_L through adjusting the set-points of generators' AVRs or shunt capacitors to change ΔQ_G. The dynamics during the set-points adjustment of primary controllers are ignored by assuming primary control is able to stabilize the dynamics fast enough in comparison the relatively slower secondary control process. Let $\Delta V_L = E_L[k+1] - E_L[k]$, $Z_{LL} = M$, $\Delta Q_L = Q_L[k+1] - Q_L[k]$, $Z_{LG} = N$ $\Delta Q_G = u[k+1] - u[k]$ so equation (3) becomes:

$$E_L[k+1] - E_L[k] = M(Q_L[k+1] - Q_L[k]) + N(u[k+1] - u[k]) \tag{4}$$

In this discrete time domain model, dynamics of load voltages are externally driven by disturbances $Q_L[k+1] - Q_L[k]$ and control $u[k+1] - u[k]$. Usually, in electric power systems the number of control generators are much smaller than the number of loads so the matrix N is a non-square matrix with the number of rows much more than the number of columns. To design the control, it is impossible to inverse N and let the control totally cancel the effectiveness caused by the disturbances. Complementary effort should be made to limit the voltage deviations systematically. In the work of this report, a linear feedback control law is used to design the secondary control, the same as in [15].

$$u[k+1] - u[k] = \sum_{j=1}^{p} (E_{Lj}[k+1] - E_{Lj}[k]) v_j \tag{5}$$

where p is the number of pilot-points which have PMUs as measurement. $E_{Lj}[k+1] - E_{Lj}$ is the voltage deviation on the jth pilot-point. v_j is the feedback control gain corresponding to the voltage deviation information from the jth pilot points. Before the control is applied, voltage deviations on pilot buses are driven by disturbances only:

$$E_{Lj}[k+1] - E_{Lj}[k] = M_1 \Delta (Q_L[k+1] - Q_L[k]) \tag{6}$$

where M_1 is the rows of Z_{LL} corresponding to the monitored pilot buses.

There is another important and appropriate assumption that during two short-term intervals, in electric power systems the reactive power disturbance will not increase or decrease too much and the increment stays in a upper bound. The mathematical form of this assumption is:

$$\|Q_L[k+1] - Q_L[k]\|_\infty \leq \gamma \tag{7}$$

Recall that the objective of control is to limit the voltage deviations systematically, the L_∞ norm minimization of the $E_L[k+1] - E_L[k]$ is used to design the feedback control gains.

$$\min_{v_1,v_2,...,v_p} \left(\max_{\|Q_L[k+1]-Q_L[k]\|_\infty \le \gamma} \|M(Q_L[k+1] - Q_L[k]) + N[v_1, v_2, ..., v_p]M_1(Q_L[k+1] - Q_L[k])\|_\infty \right) \tag{8}$$

which equals to

$$\min_{v_1,v_2,...,v_p} \gamma \|M + N[v_1, v_2, ..., v_p]M_1\|_\infty \tag{9}$$

The L_∞ norm of a matrix is defined as the maximal absolute value of the summation of each row of this matrix. In order to obtain better control performance, we re-set the objective function (9) to limit every entry of the matrix.

$$\min_{v_1,v_2,...,v_p} \gamma \|M + N[v_1, v_2, ..., v_p]M_1\|_{max} \tag{10}$$

where

$$\|A\|_{max} = \max_{i,j} |a_{ij}|. \tag{11}$$

Let m_j^T represent the jth row of M and n_j^T represent the jth row of N. The jth row of the matrix in (10) is then

$$r_j^T = m_j^T + [n_j^T v_1, n_j^T v_2, ...n_j^T v_p] \begin{bmatrix} m_1^T \\ m_2^T \\ \vdots \\ m_p^T \end{bmatrix} \tag{12}$$

Transpose (12) and recognize that the max norm of the matrix in (10) is equivalent to the L_∞ norm in $R^{m\times 1}$.

$$\min_{v_1,v_2,...,v_p} \gamma \left\| \begin{bmatrix} m_1 \\ m_2 \\ \vdots \\ m_l \end{bmatrix} + \begin{bmatrix} m_1 n_1^T & m_2 n_1^T & \dots & m_p n_1^T \\ m_1 n_2^T & m_2 n_2^T & \dots & m_p n_2^T \\ \vdots & \vdots & \vdots & \vdots \\ m_1 n_l^T & m_2 n_l^T & \dots & m_p n_l^T \end{bmatrix} \begin{bmatrix} v_1 \\ v_2 \\ \vdots \\ v_p \end{bmatrix} \right\|_\infty \tag{13}$$

Equation (13) is the objective function for designing the control gains of robust AVC with information from pilot-points measurement. Usually, system operators take a small number of pilot-points out of the whole load buses to represent the voltage situation of the whole control area; and the number of control generators is also much smaller than the total number of loads to be controlled. The selection of an optimal set of control gains vectors v_j is then equivalent to the

solution of an over-determined set of equations in the Chebyshev sense. The number of equations in (13) is l^2 where l is the number of load buses and the number of unknowns is cp where c is the number of control generators and shunt capacitors and p is the number of pilot-points. The solution to (13) only need to be evaluated off-line for various choices of pilot-points and the results corresponding to different combinations of pilot-points will only be compared off-line also.

Based on the problem that is proposed above, a special case needs to be taken into consideration. It is for future smart grid, PMUs might be installed at every bus of the transmission power grid, or the number is large enough to guarantee the full observability on bus voltages and phase angles of each control area. This indicates that in equation (6), the voltage deviations caused by $Q_L[k+1] - Q_L[k]$ could be fully monitored. An obvious control strategy is then to select a control to minimize the maximum voltage deviation, i.e.

$$\min_{u} \ \|M(Q_L[k+1] - Q_L[k]) + N(u[k+1] - u[k])\|_\infty \tag{14}$$

Since this control design is based on the complete information structure in the sense that all load bus voltages must be monitored and communicated to the control center where (14) is solved in the center computer. The solution should then be communicated to each controller with the information that by how much it is asked to change the set-points of its primary voltage control. The solution and performance of (14) could be considered as a benchmark to compare with the solution and performance of the less information cases.

3.2 Illustration of the AVC Design on a Small 5-bus Electric Power System

In this section, the proposed robust AVC is illustrated on an example of 5-bus power system (Figure 1).

In this system, let load 5 have reactive fluctuation around the nominal point. The robust AVC could be stated as a question that whether the fast measurement PMU should be installed at load 4 or load 5 to send feedback information of the pilot point to control generators G1, G2 and G3. In the limited information case, the feedback control gains of each generator is designed by solving the optimization problem (13). Results from the alternative cases that the PMU is installed at load 4 or load 5 are then compared to get the optimal option of pilot point. One should keep in mind that these are all off-line design. When the voltage deviations happen to the load buses because of the disturbances on load 5, pilot-point voltage deviation will be measured by the installed PMU and

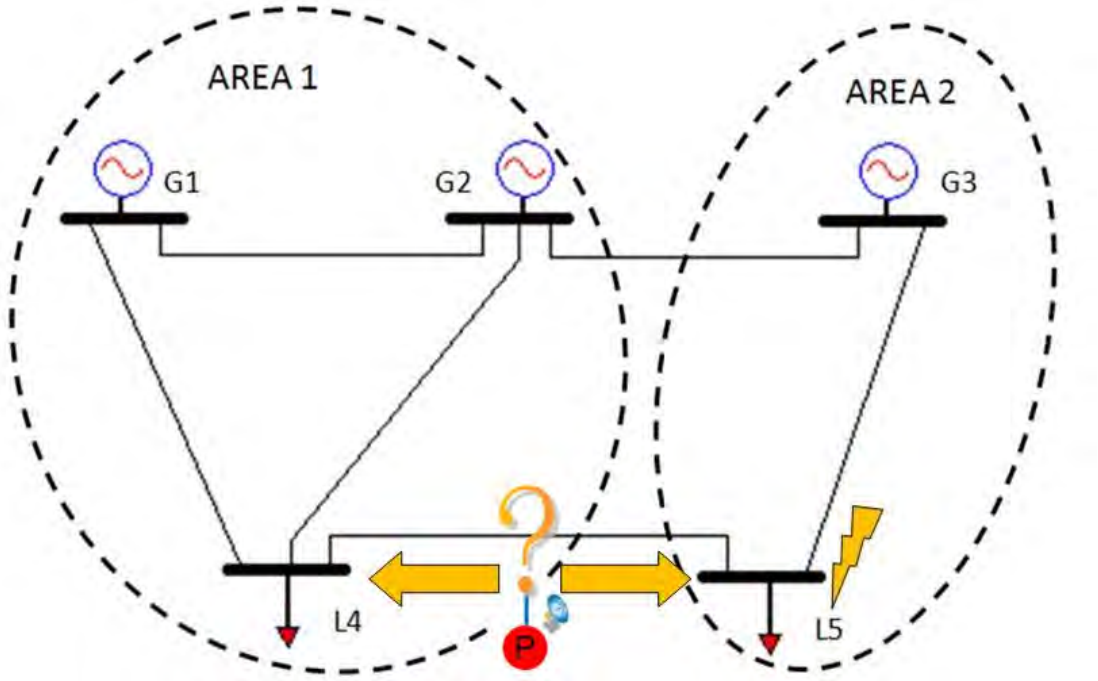

Figure 1: PMU-based AVC on 5-bus Power System

sent to G1, G2 and G3 directly. With the pilot point information, according to the pre-designed control gains, the control generators will adjust their set-points of primary voltage controller AVRs based on (5). In the complete information case with PMUs on both load 4 and 5, in each time step of applying the control, load voltage deviations resulted from $Q_L[k+1] - Q_L[k]$ are measured and transmitted to control center where the information is further processed to design the set-points adjustment of G1, G2 and G3 on real-time. The secondary control signal is then sent to these control generators from the control center.

3.3 Transferring Control Objective Function to Linear Programming Problem

Equation (13) and (14) are the basic objective functions for robust AVC in limited information and complete information case, respectively. In both of these two cases, the minimization of L_{infty} norm is used to design the feedback control u, which is basically a convex optimization problem and has only one optimal point [17]. However, the L_∞ norm is to select the largest absolute value of a vector's element or the row summation of a matrix, so that there is no explicit mathematical way or standard form to numerically derive the solution for its optimization problem. To implement the

proposed secondary voltage control scheme more cost-effectively, equivalencing the L_∞ optimization problem into classical optimization problem such as Linear Programming (LP) becomes significant. In this report, the transferring is done as:

$$\begin{aligned} &\min_{u} \ t \\ &s.t. \\ &|w_i + n_i u| \leq t \\ &i = 1, 2, ..., l \end{aligned} \tag{15}$$

and further extracted as:

$$\begin{aligned} &\min_{u} \ t \\ &s.t. \\ &w_i + n_i u \leq t \\ &-w_i - n_i u \leq t \\ &i = 1, 2, ..., l \end{aligned} \tag{16}$$

where w_i in general stands for the ith element of the first vector in the $\|\cdot\|_\infty$ of (13) and (14). u is the vector corresponding to control. n_i stands for the ith row of the matrix that maps u to the voltage deviation in both of these two objective functions. (16) now becomes a standard LP form which is at the same time equivalent to the L_{infty} optimization problem that is proposed previously. Methods for deriving the optimal solution of this LP problem have discussed in many literatures for quite a long time [17, 18, 19], which will not be re-concerned in the work of this report.

4 PMU-based Automated Flow Control Design

In this chapter, a novel method for automated control of transmission line flow deviations in response to hard-to-predict real power load deviations is proposed. The problem formulation is similar to the problem formulation of PMU-based robust AVC above. The linearized relation of the transmission line flow deviations with respect to the disturbances in real power consumption of load buses is defined by using the well-known distribution factor matrix D_f:

$$\Delta F_{Lines} = D_f \Delta P_{Inj} \tag{17}$$

where F_{Lines} denotes the vector which contains power flow on all transmission lines. P_{Inj} is the real power injection on each bus except the reference bus. This has assumed the decoupling between reactive power problem and real power problem by the assumption that in each bus voltage is controlled at its nominal value.

Re-order the D_f so that the first part of columns is for generator buses that participate as controller and the rest is for loads and generators which contribute as sources of disturbances to the system.

$$D_f = [D_{fc} \;\; D_{fuc}] \tag{18}$$

Using this partitioning, the closed-loop interdependence of transmission line flow deviations on disturbances and controls is as follows:

$$\Delta F_{Lines} = D_{fuc}\Delta P_{PQ} + D_{fc}\Delta P_{PV} \tag{19}$$

Similar to the voltage problem described by equation (3), the flow deviations ΔF_{Lines} are caused by real power fluctuations ΔP_{PQ} of load buses and uncontrolled generators (grouping buses with uncontrolled generators as PQ buses). Secondary flow control is to adjust the set-points of control generators by ΔP_{PV} to regulate the flow deviations as much as possible to match the reliability criteria. Still, the number of generators that contribute as control is usually much smaller than the uncontrolled generators and load buses. This makes it impossible to cancel out the effectiveness caused by disturbances. Control is designed to minimize the worst case flow deviations in order to ensure the reliability systematically.

Let $\Delta F_{Lines} = F[k+1] - F[k]$, $D_{fuc} = M'$, $\Delta P_{PQ} = P_{PQ}[k+1] - P_{PQ}[k]$, $D_{fc} = N'$ and $\Delta P_{PV} = u'[k+1] - u'[k]$ and equation (19) is re-written as:

$$F[k+1] - F[k] = M'(P_{PQ}[k+1] - P_{PQ}[k]) + N'(u'[k+1] - u'[k]). \tag{20}$$

The secondary level control is designed based on the linear feedback scheme introduced in (5). The difference between the linear feedback control of robust AFC and robust AVC is that in robust AVC, measurement devices on the pilot-points provide the deviations on voltage directly; while in the robust AFC, the flow deviations are not taken as pilot measurements directly. Instead, the phase angle deviations on pilot-points are measured by PMUs as feedback information to close the control loop. The reason why the work in this report abandons flow deviations as feedback is that

currently the GPS functioned fast measurement devices such as PMUs are characterized to measure voltage magnitude and phase angle in a high speed and accuracy; also, transmission lines usually need to be tripped off periodically for the needs of maintenance, which may cause troubles of loss of information for secondary control when some pilot lines are under maintenance. To use the phase angle deviation of pilot buses as feedback control information is applicable because in real power problem, power flow on transmission lines, power injection on buses and phase angle of buses are tightly coupled with each other. Such a control is:

$$u'[k+1] - u'[k] = \sum_{j=1}^{p'} (\delta_j[k+1] - \delta_j[k]) v'_j \tag{21}$$

where δ_j is the phase angle measured on the jth pilot-point. It includes both the PV and PQ buses because unlike robust AVC with fixed voltage on control generators, the change in phase angles with respect to real power disturbances is a global phenomena, which means both phase angles of both PV and PQ buses could be impacted by disturbances. So every bus excluding the reference bus is potential to be selected as pilot-point.

To relate the phase angle deviations of pilot-points with respect to the disturbances of PQ buses, we use the decoupled sensitivity matrix H_1 of real power flow (inverse of the Jacobian matrix):

$$\delta_j[k+1] - \delta_j[k] = H_1(P_{PQ}[k+1] - P_{PQ}[k]) \tag{22}$$

By substituting equations (22) and (21) into (20), the L_∞ optimization problem is designed to obtain the optimal control gains.

$$\min_{v'_1, v'_2, ..., v'_p} \Big(\max_{\|P_{PQ}[k+1] - P_{PQ}[k]\|_\infty \leq \beta} \|M'(P_{PQ}[k+1] - P_{PQ}[k]) + N'[v'_1, v'_2, ..., v'_p] H_1 (P_{PQ}[k+1] - P_{PQ}[k])\|_\infty \Big) \tag{23}$$

$\|P_{PQ}[k+1] - P_{PQ}[k]\|_\infty \leq \beta$ is the assumption adopted to this objective function from (8). Through the same derivation of (8) to (13), the equivalenced objective function of robust AFC could be then posed as:

$$\min_{v'_1, v'_2, ..., v'_p} \beta \left\| \begin{bmatrix} m'_1 \\ m'_2 \\ \vdots \\ m'_r \end{bmatrix} + \begin{bmatrix} h_1(n'_1)^T & h_2(n'_1)^T & \dots & m_p(n'_1)^T \\ m_1(n'_2)^T & m_2(n'_2)^T & \dots & m_p(n'_2)^T \\ \vdots & \vdots & \vdots & \vdots \\ m_1(n'_r)^T & m_2(n'_r)^T & \dots & m_p(n'_r)^T \end{bmatrix} \begin{bmatrix} v'_1 \\ v'_2 \\ \vdots \\ v'_p \end{bmatrix} \right\|_\infty \tag{24}$$

in which the r stands for the number of rows of matrix M', the same as the number of transmission lines.

The full information special case is also considered in AFC problem that for future smart grid fast measurement units may be installed at every bus in the electric power system. As a result, the system operator would obtain the observability of the states on each transmission line. With the flow deviations $F[k+1]-F[k]$ fully monitored, the secondary control could be designed on real-time to minimize the system-wide worst transmission line power flow deviations.

$$\min_{u} \ \|M'(P_{PQ}[k+1]-P_{PQ}[k])+N'(u'[k+1]-u'[k])\|_{\infty}. \tag{25}$$

In this case, flow deviations before secondary control is taken into action is resulted from the disturbances $M'(P_{PQ}[k+1]-P_{PQ}[k])$ only. They are all measured by PMUs and sent to the control center for designing secondary control on real-time. Control signal is then transmitted to each participating generator to adjust its set-point of primary real power control. The same as the complete information problem (14) in AVC, (25) could also be regarded as a benchmark comparison with the solution and control performance of the less information cases.

4.1 Illustration of the AFC Design on a Small 5-bus Electric Power System

In this section, robust AFC propsed in this chapter is illustrated by again using the 5-bus power system (Figure 2).

In this system, let load 5 have real power fluctuation around the nominal point. The robust AFC could be stated as a question that whether the fast measurement PMU should be installed at G2, G3, load 4 or load 5 to send feedback information of the pilot point to control generators G2 and G3. G1 is not participating since the algorithm is established on the basis of distribution factor D_f which excludes the reference bus (the role of G1 in this 5-bus example). The optimization problem (24) is solved off-line for limited information case to select the best location of the PMU by considering different options (on load 4 and 5) and comparing the results. Phase angle of the selected pilot-point is measured by the PMU and sent to control generators G2 and G3 when secondary control is needed. After receiving the signal of phase angle deviation, G2 and G3 will then adjust their set-points of real power primary control based on (21). For the complete information case, power flow deviations on all of the 6 transmission lines are monitored by PMUs which have been installed on the two ends of each transmission line. By solving (25) on real time given the measurement from PMUs,

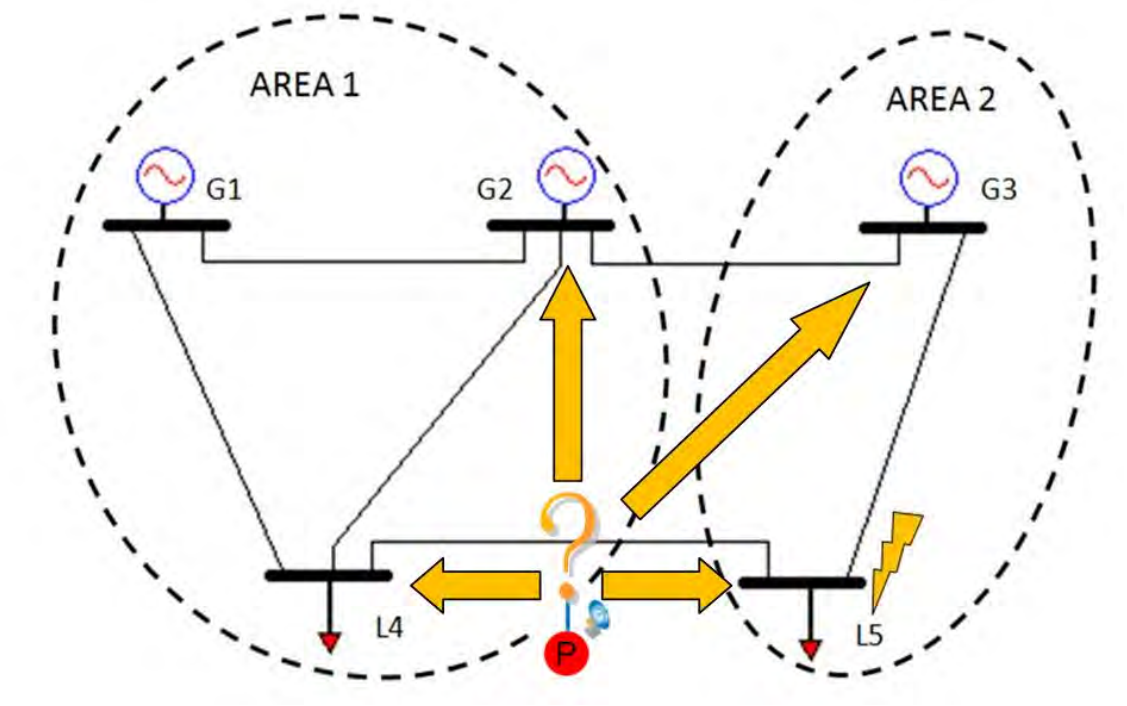

Figure 2: PMU-based AFC on 5-bus Power System

the optimal control signals for G2 and G3 are obtained and sent them through communication channels. There is an obvious increasing of measurement devices and communication channels from the limited information case to the complete information case, and in order to monitor the whole set of transmission lines, even PV buses need to install PMUs. This problem needs to be addressed for the cost-effectiveness of a secondary control infrastructure with given number of PMUs.

4.2 Transferring Control Objective Function to Linear Programming Problem

In this section, the optimization problems in (24) and (25) are transferred into LP problems with the same approach discussed in section (3.3). The standard LP form for these two optimization problems is:

$$
\begin{aligned}
&\min_{u'} \ t' \\
&s.t. \\
&w'_i + n'_i u' \leq t' \\
&-w'_i - n'_i u' \leq t' \\
&i = 1, 2, ..., r
\end{aligned}
\tag{26}
$$

where w'_i in general stands for the ith element of the first vector in the $\|\cdot\|_\infty$ of (24) and (25). u' is the vector corresponding to control. n'_i stands for the ith row of the matrix that maps u' to the voltage deviation in both of these two objective functions. r is the number of transmission lines being regulated.

5 A Multi-Layered Clustering Algorithm for Determining Secondary Control Zones

A possible implementation of robust AVC or AFC for large-scale systems raises several questions concerning basic communication and control architecture. The choice of architecture determines the underlying computational complexity. There are two basic approaches. The first approach is to consider a large power system as one single control area and perform off-line optimization to determine the best locations for a given number of PMUs; control gains are computed assuming all controllers communicate with the PMUs. The second approach is to consider a large electric power system as an interconnection of several weakly connected subsystems. The best locations and control gains are computed for each subsystem separately as a stand alone system. This is again similar to the AGC in which each control area responds to its own imbalances by controlling its own resources. However, the AVC problem for large-scale system is generally more complicated because it requires decomposing the system into reactive power control zones according to the electrical characteristics of the transmission system. Moreover, voltage deviations within a zone are generally more locally characterized than the frequency deviations within a control area. Because of this there is a definitive challenge of selecting the most effective locations for the voltage measurements for each reactive power zone. For the AFC problem, in the work of this report, it is intending to use the first approach mentioned before because the objective of AFC is to regulate the transmission

line flow deviations so to cluster the large system into several groups of buses and let each group control its own flow deviations in secondary level will definitely lose the control on tie-lines that interconnect the subsystems together. The regulation on interconnection tie-line flows is actually concerned a lot by power engineers and even part of the function of AGC is to compensate the effectiveness of tie-line flow deviations around the pre-scheduled operating point. Consequently, in AFC, controlling the tie-line flow deviations cannot be ignored and it's better to consider the as one control area.

5.1 Numerical Problems With A Single-Layer Clustering Algorithm

In this section we introduce a new algorithm for clustering a large-scale system into reactive power zones. Once these are computed, the method for selecting best PMU measurements in each control area is used based on the algorithm described above. The proposed algorithm draws on the early work in [20] and [21]. The algorithm in [21] is applied to the decoupled reactive power Jacobian matrix B in Equation (1). The original algorithm starts by identifying buses in each zone by finding the weakest transmission elements connected to each bus. Those transmission lines with susceptance weaker than certain pre-determined value are eliminated and groups of buses which are isolated from each other are clustered into separable zones. We refer to the original method in [21] as α clustering. In short, it comprises the following steps:

1. Choose the cutoff value α.
2. Search for the largest diagonal element of matrix B which is called d.
3. Normalize B by dividing every element by d.
4. For each row i of the normalized matrix B, rank the absolute values of the off diagonal elements from smallest to largest. Then the elements with the smallest absolute values are eliminated from each row i until the sum of eliminated elements is close to but still smaller than cutoff value α.
5. Groups of buses which are still interconnected after the weakest branches connected to each bus are eliminated form weakly connected separable reactive power zones.

This algorithm is repeated by pre-setting a table of different values for α, by trying each α from the table and selecting the decomposition which best meets the clustering specifications, such as the desired number of groups and/or number of buses,ie. size, of each group.

However the original clustering algorithm generally experiences implementation problems. In particular, the method is quite sensitive to the choice of α. If α is too large every bus becomes a subgroup; and if α is too small, the entire system is hard to be broken into pieces. To overcome this problem, we propose next a multi-layered algorithm which continues to divide the largest subgroup resulting from last clustering step until each subgroup has nearly equal size.

5.2 A Novel Numerically Stable Multi-Layered Clustering Algorithm

Typically the single-layer algorithm results, at best, in several rather large subgroups and many relatively small subgroups for any chosen α. For several implementation reasons it is much more desired to have zones of relatively similar size no larger than 100 buses or so, even for very large systems. Given this design objective, we propose the following multi-layered clustering algorithm. Each single layer subgroup is further decomposed multiple times until the desired specifications are reached. The implementation is as follows:

1. Find the largest subgroup k of the system. (At first step the largest subgroup is equal to the system itself).

2. Implementing the single layer method for the largest subgroup corresponding to a given cutoff accuracy α. This requires to select the cutoff value α and implement the single-layer clustering algorithm to group k.

3. Managing "missing buses"– The resulting sub-matrix after Step 2) may have some rows which have no off-diagonal elements which means no connection to any other bus because the α was chosen too large. These rows represent the "missing buses". This requires identifying the missing buses and determining whether they have any connections with the existing subgroups. If a specific missing bus has a connection with the existing subgroups, it gets removed from the missing bus set and integrated into the subgroup with which it has the strongest connection according to electrical distance matrix B. This generally leads to a size increase of the existing subgroups. If the missing bus has no connections to the existing subgroups, continue to find

the next missing bus which has interconnection with an existing group.

4. If the set of missing buses is empty, it means the disconnected missing buses all gets integrated to a subgroup and one could continue to next step. Otherwise, it should take a step back to 3.

5. Specify value m which defines the minimal number of buses one group should have, and compare the size of each subgroups obtained from step 4. For the groups whose size are larger than m, no further action is required. For each group whose size is smaller than m, compare the electrical distance of its connection to all existing subgroups and integrate it into the one to which it has the shortest electrical distance.

6. Check if the subgroups obtained in Step 5 meet the requirement of being of a similar size, which is to evaluate if the smallest subgroup is larger than the pre-specified minimal size. If yes, stop; if no, go back to Step 1 and repeat from 1 to 5.

Once the clustering is done, a re-numeration is done to define Jacobian matrices corresponding to each subgroup (zone). This is to simply select from the original matrix B rows and columns corresponding to each bus in the zone. Once the zonal Jacobian matrix is determined, finding the best PMUs locations and optimal control gains for each subgroup is carried out based on the algorithm introduced in Chapter 3.

6 Communication Architecture for the Implementation of PMU-based Secondary Controls

In this chapter, measurement and communication issues are discussed for the implementation of PMU-based AVC and AFC. A brief introduction to the features of PMUs is made in the beginning. Communication infrastructures are then proposed for the transmission of pilot-points PMUs measurement signals and the control signals.

6.1 Introduction to Phasor Measurement Units

Modern phasor measurement systems could trace their origin to the development of the Symmetrical Component Distance Relay (SCDR) in the early 1970s. SCDR was developed to use symmetrical

components of voltages and currents in order to convert the 6 fault equations of a three phase transmission line into a single equation because the microcomputers of that period were not capable enough to handle the requirement of a distance relay algorithm. Although the SCDR was no longer used later on as the blooming of computer technology and engineering to measure the positive sequence voltages and currents of a power grid was reserved from SCDR as the backbone of most power system analysis programs [11, 1].

In early 1980s the Global Positioning System (GPS) was deployed and provides a globally valid time reference to electric power engineering. This means that measurements taken, or phasors computed via a time reference at one location would become globally valid to be used both in local computation and the computations at other locations by sending the data through a communication link. When the number of installed GPS functioned phasor measurement devices is large enough to measure the full states of the whole power grid, with the time stamped positive sequence measurements, the system operator will be provided instantaneous pictures of the states of the power system in each updating time step.

Phasor Measurement Units (PMUs) are well-known as the representative of the GPS functioned phasor measurement devices introduced above. They use the GPS signal to synchronize the sampling clocks so that the calculated phasors would have a common time reference. With the updating frequency up to 30 Hz, sensor network that is comprised of PMUs enables the system operator to access the whole system sates on real-time. The first PMU was developed in the Power System Research Laboratory of Virginia Tech (Figure 3).

In electric power engineering, the sinusoid wave with fundamental frequency is represented as 'phasor' which has a magnitude equal to the magnitude or the root-mean-square (rms) of the sinusoid wave and a angle equal to the angle between starting time point $t = 0$ to the closest peak of the wave (shown as Figure 4). The mathematical expression of phasor is:

$$\begin{aligned} A\cos(\omega t + \delta) &= \frac{A}{2}e^{i(\omega t+\delta)} + \frac{A}{2}e^{-i(\omega t+\delta)} \\ &= Re\{Ae^{i\delta}e^{i\omega t}\}. \end{aligned} \tag{27}$$

where phasor can be simply refer to $Ae^{i\delta}$.

As it has been introduced, PMUs sample the sinusoid voltage wave and calculate its phasor based on the sampled data. The most commonly used method to calculate phasors is that of Discrete Fourier Transform (DFT) which is shown in Figure 5. The sampling clocks are usually

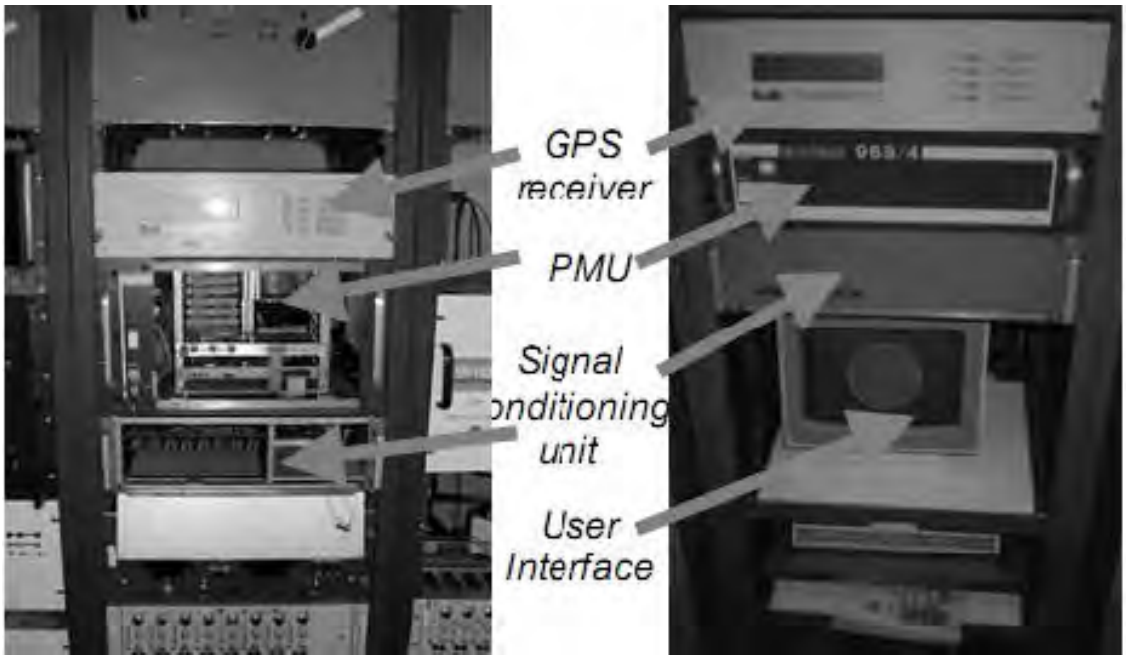

Figure 3: The First PMU Developed in Virginia Tech in 1980s [1]

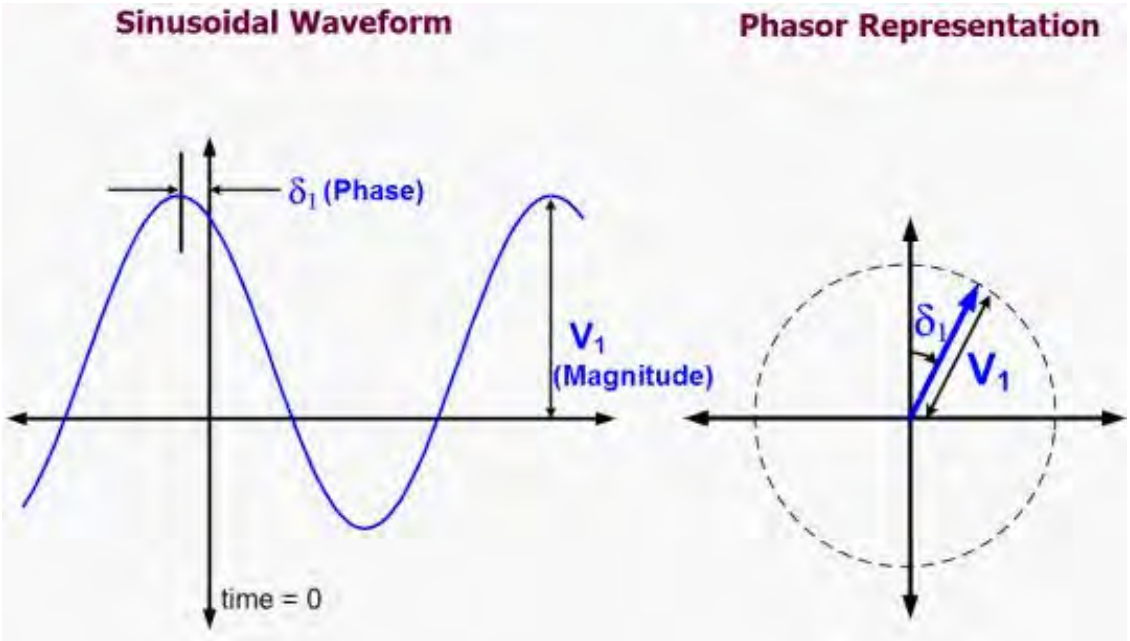

Figure 4: Illustration of Sinusoid Wave and Its Phasor Representation

kept at a constant frequency even though the input signal frequency may vary by a small increment around its nominal value. Let N to be the number of sampling and $\theta = 2\pi/N$ (θ is defined as the sampling angle in terms of the period of the fundamental frequency component). The phasor after N sampling (from 0 to N-1) is derived by summing up all of the samplings.

$$\begin{aligned} X^{N-1} &= \frac{\sqrt{2}}{N}\sum_{n=0}^{N-1} x_n(\cos(n\theta) - j\sin(n\theta)) \\ &= \frac{X_m}{\sqrt{2}}e^{j\delta} \end{aligned} \tag{28}$$

where X_m represents the magnitude of the phasor. δ is the angle of the phaosr.

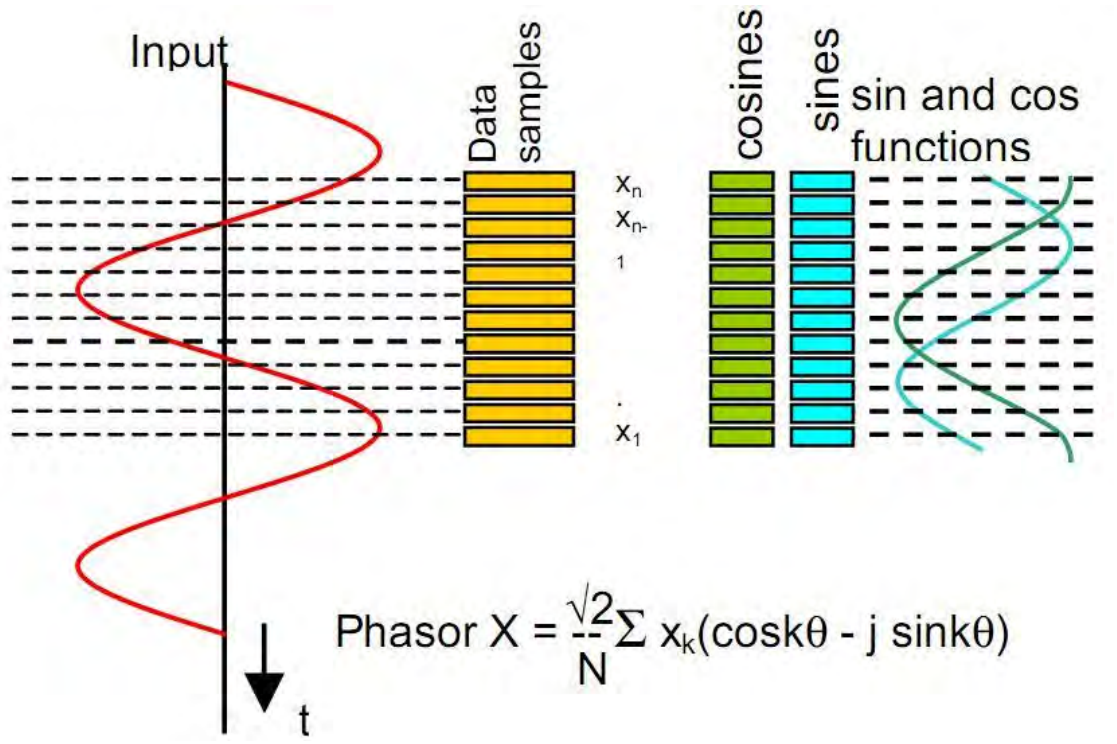

Figure 5: Estimation of Phasors from Sampled Data Using Discrete Fourier Transform [1]

6.2 Communication Architecture for Secondary Level Control in Different-Amount-of-Information Cases

In this section, the communication architectures of different types of secondary level control are proposed.

In the first place, the communication architecture of secondary level AGC is reviewed in Figure 6. With this measurement and control infrastructure, the Area Control Error (ACE) is calculated on the control center computer based on the measurement of area frequency and power flow on the interconnection tie-lines (sent through the bold dashed lines). Control signals for each participating generator is then sent from the control center through the light dashed line.

In the second place, similar to that of AGC, the communication architectures of AVC are proposed for the cases with limited information and full information respectively. In Figure 7, one pilot-point is selected throughout control area 1. Voltage deviation on that bus is measured by PMU and sent directly to the control generators, since the feedback control gains have already been designed and set up off-line. By comparison, the architecture of AVC with full information (PMUs on all load buses) is shown in Figure 8. In this case, much more measurement is needed than the limited information case. Voltage deviations on all load buses are monitored and sent to control center where the optimal control is determined on real-time. Through the communication channels from control center to control generators, the control signals are then distributed.

In the third place, the communication architectures of limited and full information AFC are proposed. As it was discussed in the beginning of Chapter 5, the measurement and control infrastructure is designed in a centralized way, in order to monitoring and control the power flow deviations on both intra-area transmission lines and inter-area transmission lines. This is the major difference between the communication architecture of AFC and AVC. Seen from Figure 9 and 10, one can learn that the measurement of pilot-point phase angle deviation is sent to control generators in the whole system, rather than any specific control area; while in the full information case, a control center computer takes the responsibility to collect the flow deviations of all transmission lines and design and send over the optimal control signal to each generator in the system.

7 Experimental Simulation Studies

The robust AVC and AFC are both applied to the equivalently reduced Northeastern Power Coordinating Council (NPCC) [22] power system model for simulation studies. The test system shown as Figure 11 has 36 buses with generator on each bus.

Define the same sets of control and disturbance sources for both AVC and AFC in Table 1 (represented in terms of bus numbers).

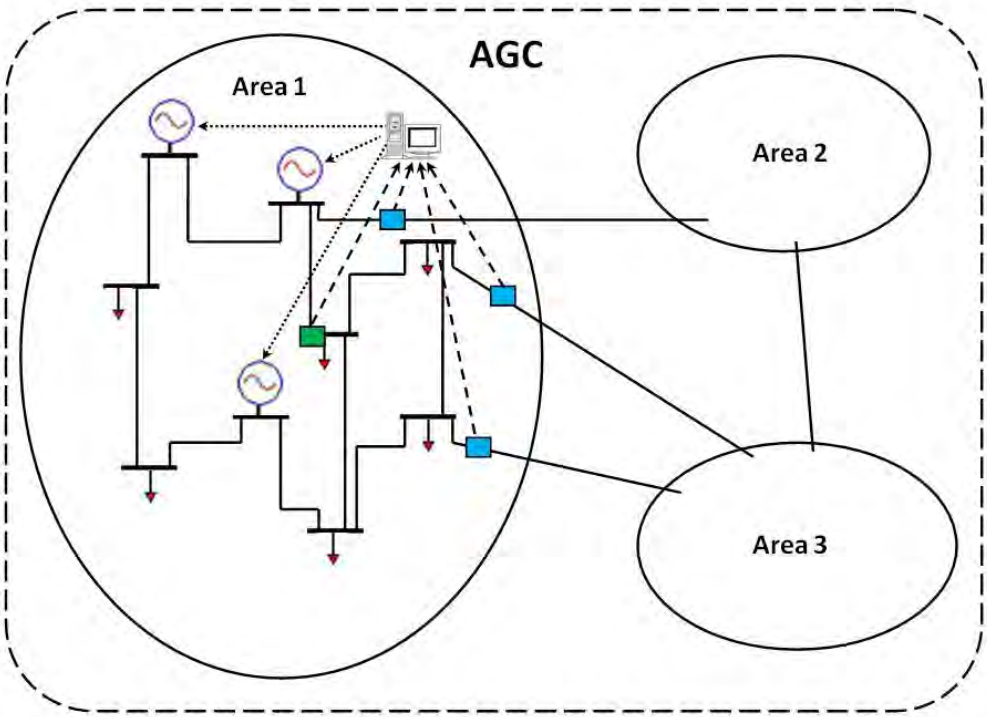

Figure 6: Communication Architecture of Conventional ACE-based AGC

Table 1: Bus-types of the Tested NPCC Power System

Control Generators (PV Buses, the Source of Control)	Under-control Buses (PQ Buses, the Source of Disturbance)
77950, 1, 75405, 79800, 74347, 74327, 79581, 70002, 71786, 71797, 72926, 73106, 73110, 87004, 80001, 80031	5028, 73171, 73663, 74316, 74341, 74344, 75050, 75403, 76663, 77400, 77406, 78701, 78702, 79578, 79583, 79584, 80101, 80121, 81615, 84819

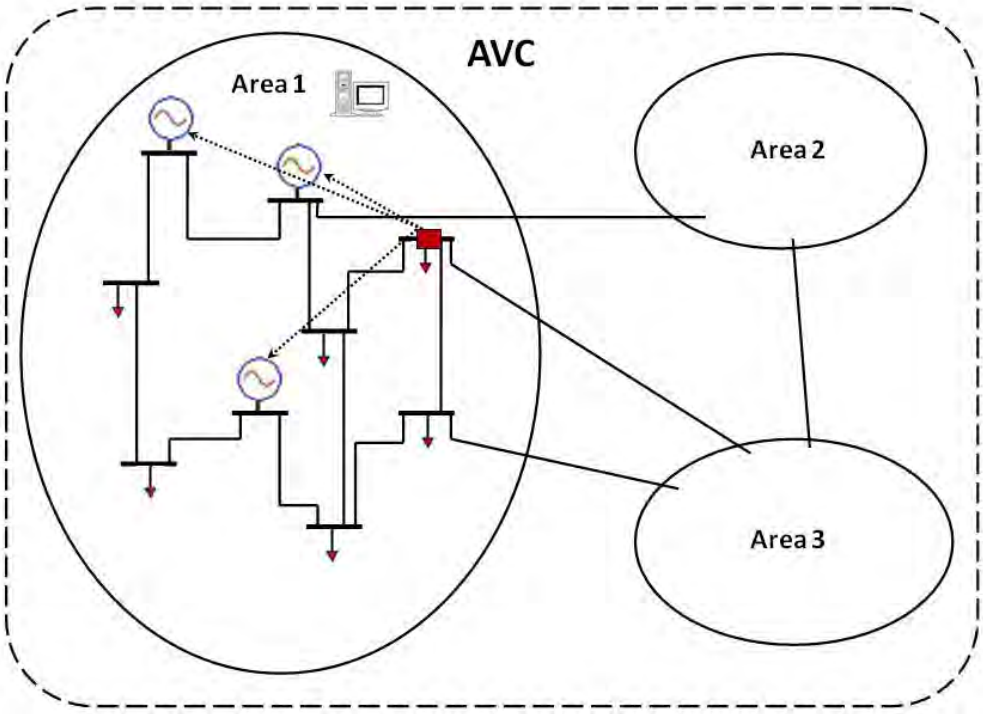

Figure 7: Communication Architecture of AVC with Limited Information

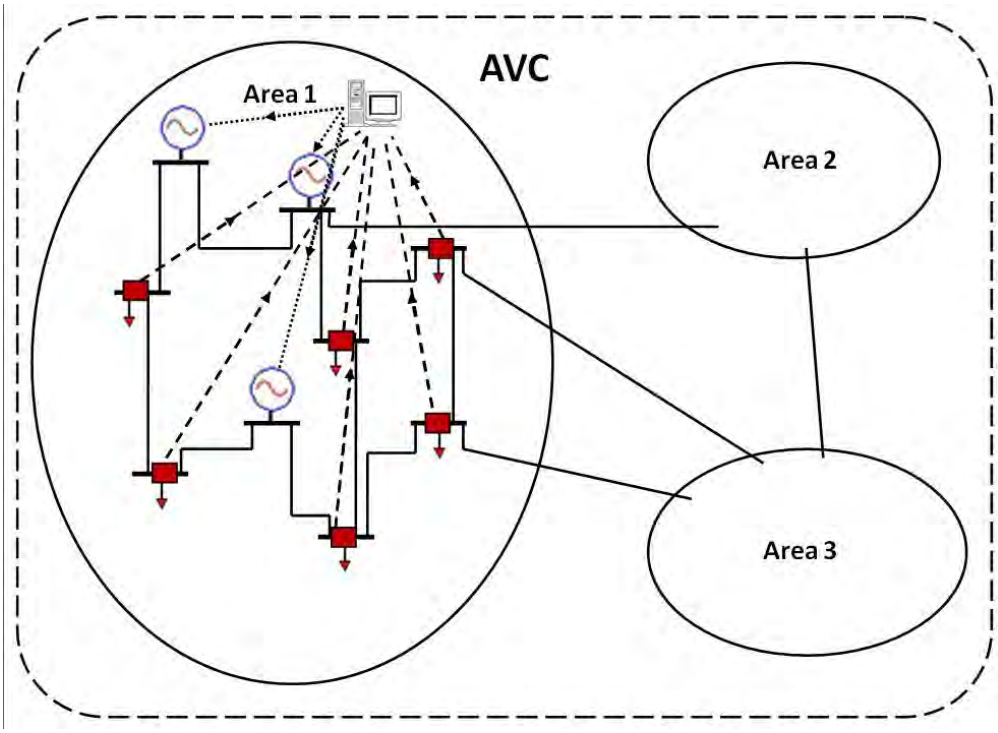

Figure 8: Communication Architecture of AVC with Full Information

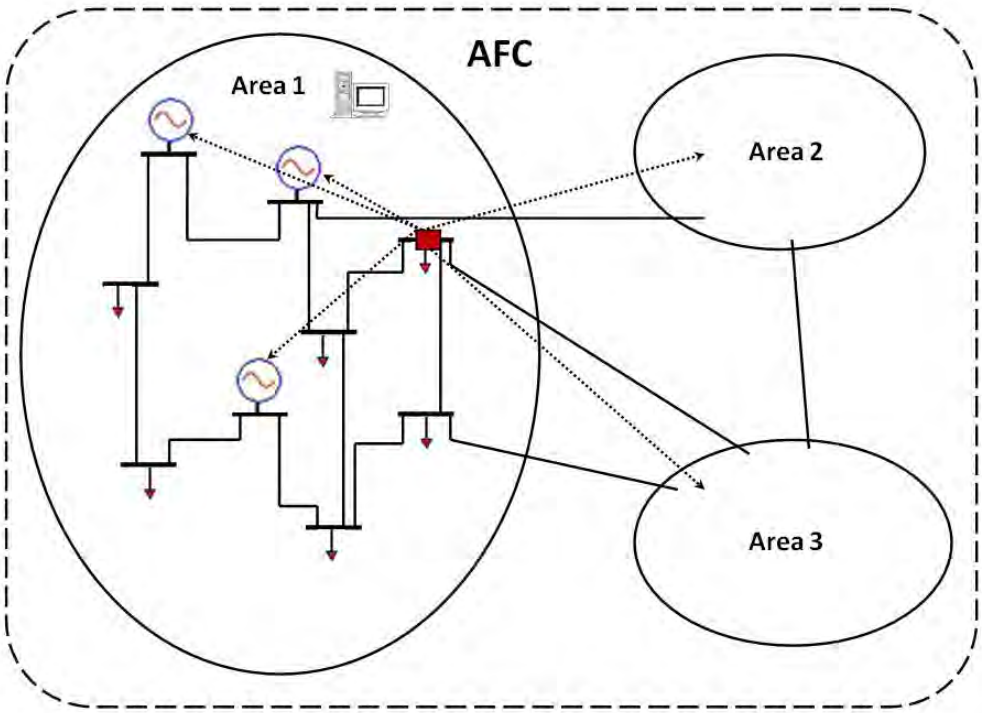

Figure 9: Communication Architecture of AFC with Limited Information

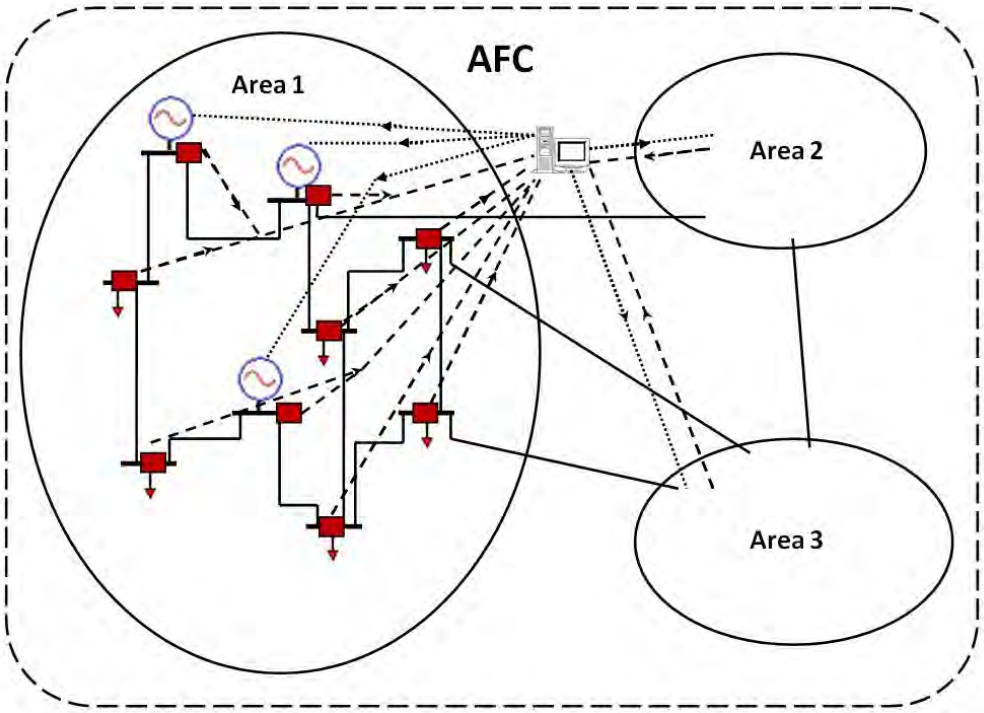

Figure 10: Communication Architecture of AFC with Full Information

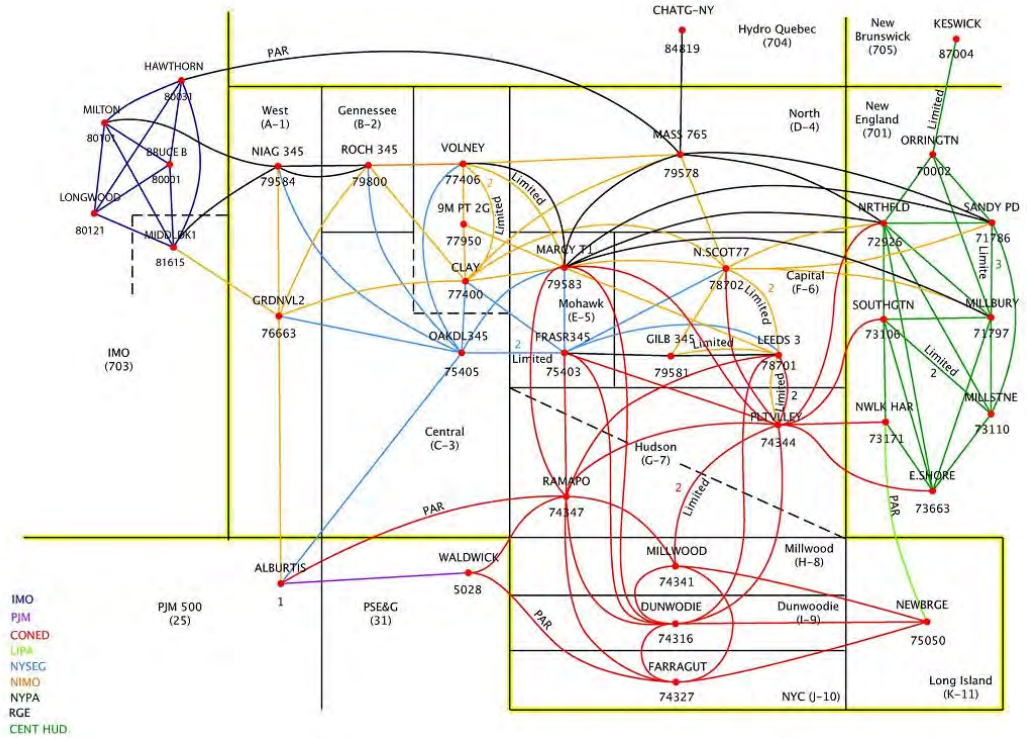

Figure 11: One Line Diagram of the Equovalenced NPCC 36-bus Power System

7.1 Simulation Studies of Robust AVC on NPCC Power System

To test the robust AVC, disturbances which satisfy the Guassian Distribution (with 0 mean and 1 variance) are applied to all of the under-control buses in each time step. System with 1 or 2 pilot points for the limited information case is studied separately. Best locations of pilot-points and the accordingly determined optimal control gains are listed in Table 2. Secondary voltage control is done by adjusting the set-points of reactive power output in every 1 second.

Table 2: Pilot-points Locations and Optimal Control Gains for the Robust AVC in NPCC System

	One Pilot-point Case	Two Pilot-points Case	
Pilot-Points	84819	76663	74316
	-9.9649	5.4075	-1.8910
	-233.0749	-90.3935	79.3448
	-40.2326	12.9060	-27.6816
	41.2642	-35.1306	35.2771
	201.0228	83.7581	-86.3241
Optimal	15.3564	-4.1015	-9.1980
Control	58.7163	-16.4325	28.7537
Gains	-338.4963	-129.8559	-109.4231
	-473.1144	-215.6334	-148.0765
	336.6767	-34.8111	84.4063
	151.8212	256.1425	23.9141
	-527.0534	71.3323	-297.4287
	645.4015	29.5126	317.2308
	-338.0668	-129.8559	-109.4231
	-28.9580	-11.6049	10.5291
	11.6139	3.3268	-1.8613

In Figure 12, the 1 and 2 pilot-points limited information case and the full information case are shown together. Through comparison among these cases with different amount of information of the system, the black curve shows the benchmark of the robust AVC with each load bus monitored by PMU. During every control step, the full information control is able to regulate the system-wide

worst voltage deviation within the ±5% criteria. While in the limited information case, 2 pilot-points control (red curve) performs worse than the benchmark but much better than 1 pilot-point case (dark green curve). It is obvious to conclude that if the system is considered as one control area without clustering, the more information provided to AVC, the better it will perform.

In the following experiment, the NPCC system is clustered into 3 sub-systems by using the Multi-layered Clustering Algorithm proposed in section 5.2. Result is shown in Figure **??**. It supports the verification of the clustering algorithm because buses in each sub-system are geographically located close to each other, which is consistent to the localized characteristic of reactive power and voltage problem. Secondary voltage control is re-designed based on the structure which has 3 sub-systems. For every subsystem, pilot-point and optimal control gains are determined by solving (16) separately. In the simulation studies of this report, 1 PMU is assigned to each area, which means the whole system has had 3 PMUs installed. Figure 14 presents the control performance. Comparison between Figure 12 and 14 indicates that even with less PMUs, control designed by considering the NPCC power system as 1 control area gives better results than the one which considers the system as 3 subsystems through clustering. One reason of this might be the electrical distances between interconnected buses are all close to average. So ignoring some relatively weaker interconnections the 3 subsystems actually lose much mutual impact in between. Since the control gains for each area are independently designed but when they are applied to control the real-time voltage deviations the system itself is still running as a whole, ignoring interconnections which are relatively weak but in fact not weak enough may cause the sub-optimal design of control gains. As a result, the clustering-based control with sub-optimal control gains would be performing worse than the control that takes the system as 1 area. At this point, more work needs to be done to apply the clustering-based control to other test systems with larger-scale than NPCC.

7.2 Simulation Studies of Robust AFC on NPCC Power System

To study the implementation of the robust AFC on NPCC power system, Guassian disturbances with 0 mean and 0.01 variance are applied to the PQ buses in each time step also. Smaller variance is used here than the test for robust AVC because power flow deviations on tie-lines are much more sensitive to load disturbances than voltage. In order to limit flow deviations within the ±5% reliability criteria, AFC is supposed to be operated before the magnitude of disturbance increases

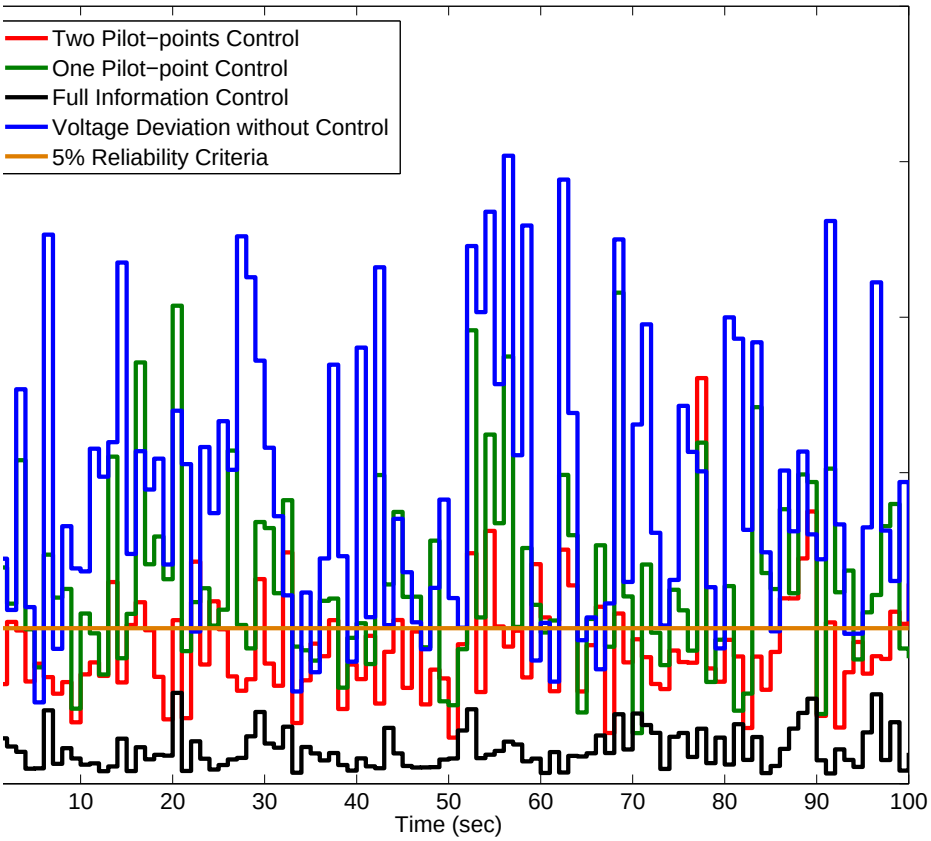

Figure 12: Robust AVC Applied to NPCC in both Limited and Full Information Cases

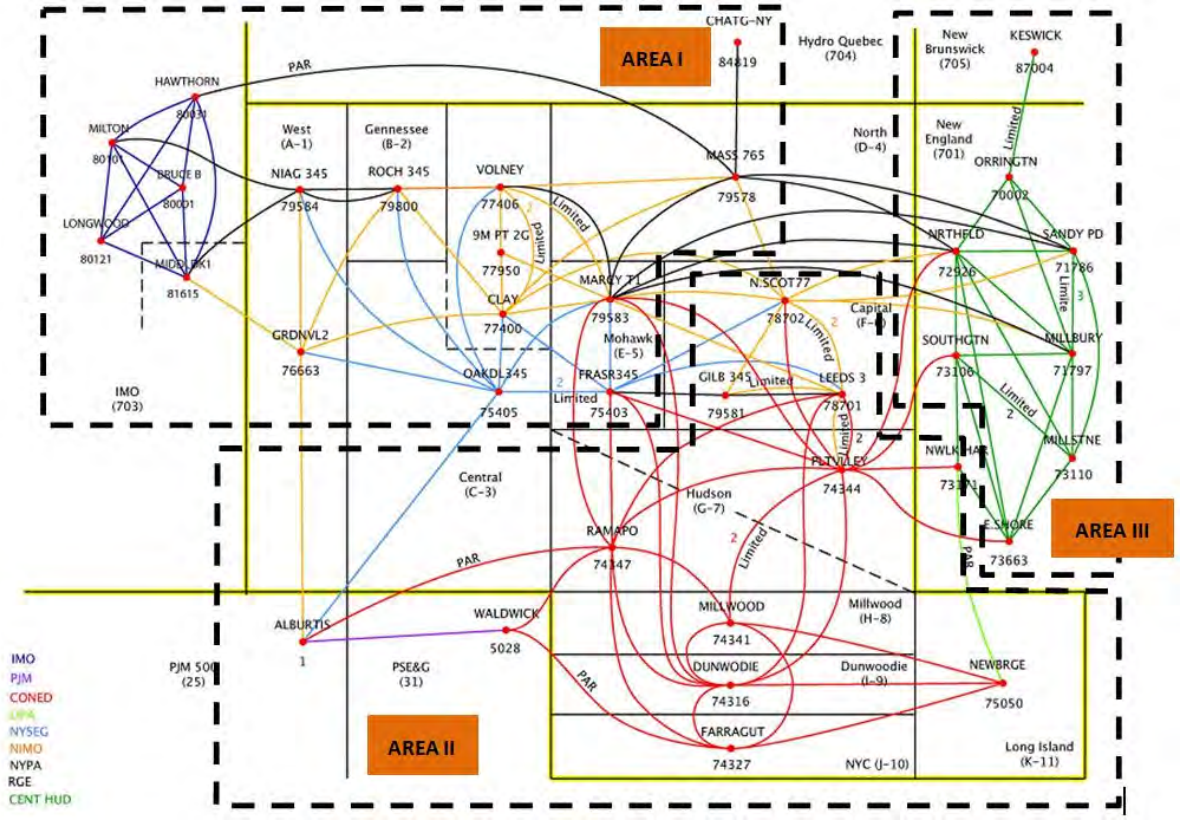

Figure 13: The Multi-layered Clustering Algorithm Applied to NPCC Power System

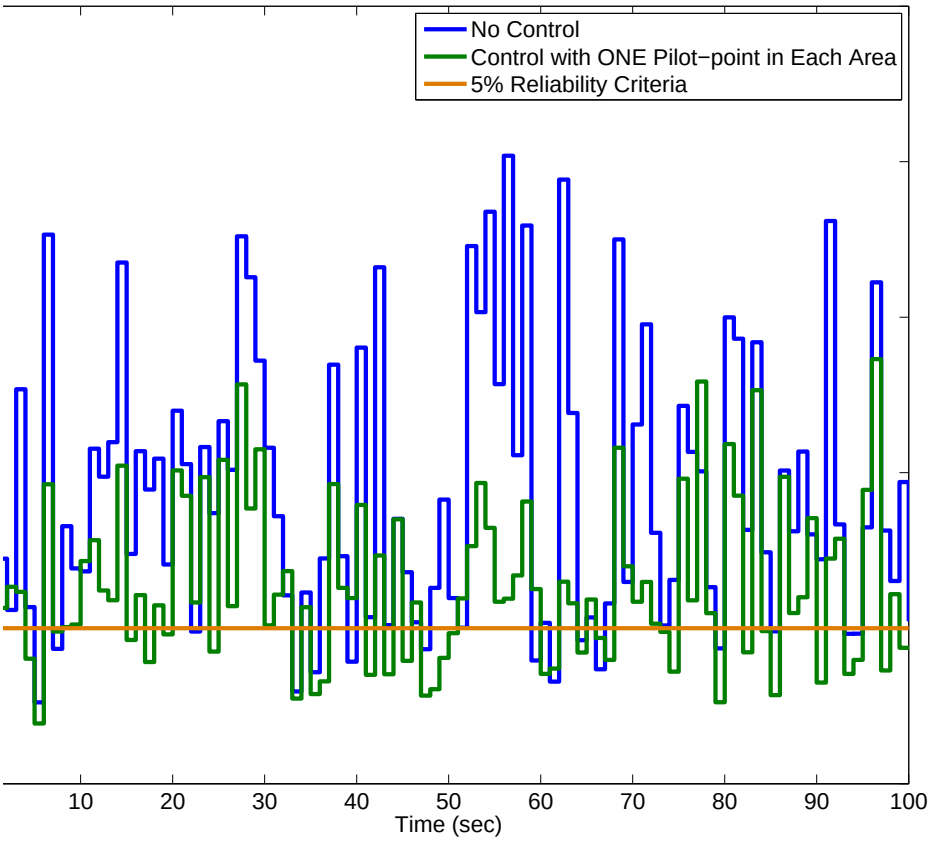

Figure 14: Robust AVC Applied to NPCC after Clustering

to a small tolerance value. In this case of study, the control is activated in every second. By solving (26) with different combinations of pilot-points, best locations of PMUs and the optimal control gains are designed. The results are demonstrated in Table 3 and Figure 12. It does not show much improvement achieved from the most limited information case (1 pilot-point) to the complete information case (all buses taken as pilot-points). This indicates a cost-effective way of applying the robust AFC. With a small number of PMUs installed on the pilot-points, the close-loop secondary control performance could be close to the benchmark; while much less effort has to be put the communication architecture. Also, more work needs to be done to verify the capability of the AFC in regulating power flow deviations on power systems with larger-scale than NPCC.

Table 3: Pilot-points Locations and Optimal Control Gains for the Robust AFC in NPCC System

	One Pilot-point Case	Two Pilot-points Case	
Pilot-Points	77406	75403	77406
	-11.3918	8.4138	-6.1413
	25.9149	3.9036	-0.2770
	15.1789	4.9733	-5.4944
	-7.5338	-7.3872	-18.0375
	-11.4397	1.4622	-3.2048
Optimal	2.1830	0.6560	-0.3949
Control	-26.7827	2.7586	-6.4526
Gains	-1.6857	-1.1376	-0.4614
	-4.6764	3.3680	-9.2431
	18.8971	-0.1432	-2.9481
	-2.1021	3.1767	-5.0220
	1.0401	14.8947	5.7579
	-13.4725	5.6898	-4.9717
	7.9034	3.7636	-1.2857
	-32.7192	3.3359	1.5321

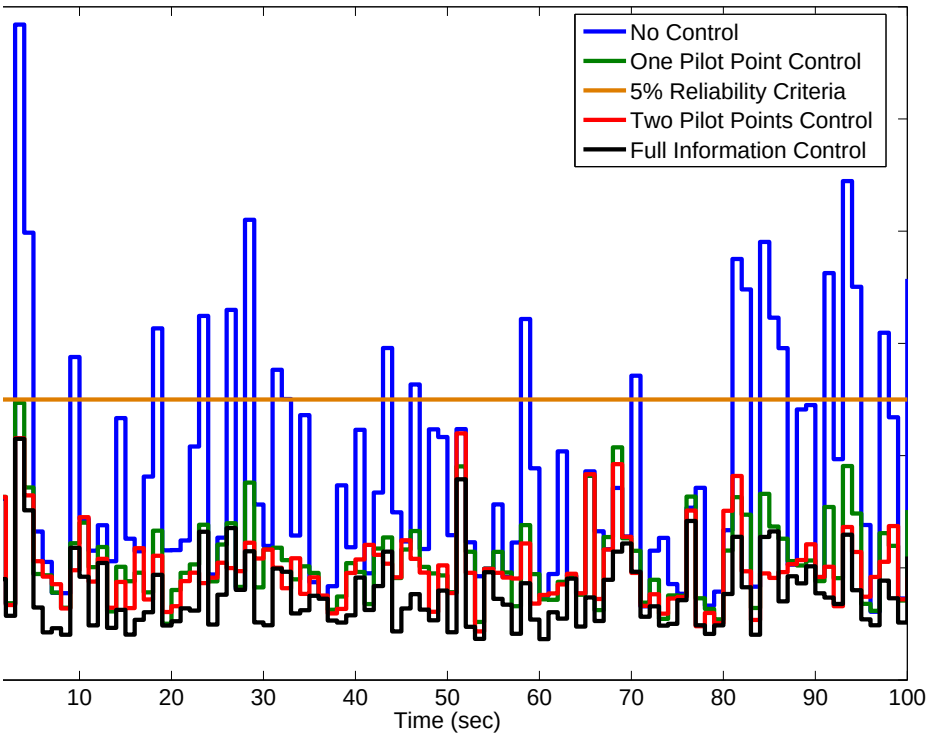

Figure 15: Robust AFC Applied to NPCC in both Limited and Full Information Cases

8 Conclusions

8.1 Contributions of This Report

This report presents the first work of using PMUs to design robust AVC and AFC to compensate hard-to-predict disturbances in secondary level. Both methods are based on the minimization of L_∞ norm in order to regulate the system-wide worst deviations of load voltages and transmission line power flows. To solve the objective functions effectively, they have been equivalently transferred into Linear Programming problems which have had well developed algorithms to find the optimum. A novel multi-layer clustering algorithm is proposed to decompose a large-scale system into several small but close-sized control areas for the robust AVC because of the localized characteristic of reactive power and voltage problem. However, the robust AFC is intending to take the centralized scheme without clustering since decomposition may cause the loss of the system structure which actually needs to be concerned significantly. Measurement and communication architectures are designed for AVC and AFC with feedback information provided by PMUs. The architectures are different between the limited information case and complete information case. In the complete information case which is corresponding to a benchmark secondary control algorithm, much more efforts should be put on building the measurement and communication infrastructure than the limited information case. This cost needs to be considered together with the performance in control side to decide a cost-effective solution for the AVC and AFC implementation in real power grid.

The idea and problem of these robust AVC and AFC are roughly illustrated in a 5-bus small power system. Simulation studies on the application to a highly aggregated NPCC power system model show more detail about the performance and potential of those two secondary controls. In the centralized way, the performance of AVC gets improved by increasing the number of installed PMUs; while the AFC is able to ensure the reliability criteria with only 1 PMU and does not get much improvement by increasing the amount of measurement. This is again because of the localized characteristic of reactive power problems and globalized characteristic of real power problems. Since it is localized, AVC needs more PMUs to be allocated on different sub-area of the system. By contrast, to deal with the globalized real power problem, AFC only needs a little information to design a well performed system-wide control.

8.2 Future Work

As it was mentioned in the context of this report, one future work would be to test the PMU-based robust AVC and AVC on actual utility systems. Much the same way as with AGC, once the manageable zones and the right output variables and control gains are designed, the size of the system is not critical. Moreover, larger-scale system with several weakly interconnected sub-areas is an applicable test field for the multi-layered clustering algorithm. Comparison could be made between the decentralized controls based on the natural control zones and the control zones given by the clustering algorithm proposed in this report. Serious effort will be needed to obtain the data, and set up the measurements in the field ultimately to verify their performance.

In longer-term, we see that the use of AVC and AFC, could have potential savings in the amount of spinning reserve necessary to meet the $(N-1)$ reliability criteria. The future work also is planned to study the effectiveness of applying multiple PMUs measurements per each zone, and to explore whether it would be possible to generalize these schemes for managing line contingencies.

Bibliography

[1] A.G. Phadke and J.S. Thorp. History and applications of phasor measurements. In *Power Systems Conference and Exposition, 2006. PSCE '06. 2006 IEEE PES*, pages 331 –335, 29 2006-nov. 1 2006.

[2] Final report on the august 14, 2003 blackout in the united states and canada: Causes and recommendations. Technical report, U.S.-Canada Power System Outage Task Force, April 2004.

[3] Interim report of the inverstiagtion committee on the 28 september 2003 blackout in italy. Technical report, Union for the Coordination of Tranmission of Electricity (UCTE), Oct. 3 2003.

[4] Marija Ilic and Shell Liu. *Hierarchical power systems control: its value in a changing industry.* Springer, London, 1996.

[5] A. Conejo and M.J. Aguilar. Secondary voltage control: nonlinear selection of pilot buses, design of an optimal control law, and simulation results. *Generation, Transmission and Distribution, IEE Proceedings-*, 145(1):77–81, Jan 1998.

[6] A. Stankovic, M.D. Ilic, and D. Maratukulam. Recent results in secondary voltage control of power systems. *Power Systems, IEEE Transactions on*, 6(1):94–101, Feb 1991.

[7] M.D. Ilic, Xiaojun Liu, G. Leung, M. Athans, C. Vialas, and P. Pruvot. Improved secondary and new tertiary voltage control. *Power Systems, IEEE Transactions on*, 10(4):1851–1862, Nov 1995.

[8] P. Lagonotte, J.C. Sabonnadiere, J.-Y. Leost, and J.-P. Paul. Structural analysis of the electrical system: application to secondary voltage control in france. *Power Systems, IEEE Transactions on*, 4(2):479 –486, may 1989.

[9] J. P. Paul, J. Y. Leost, and J. M. Tesseron. Survey of the secondary voltage control in france : Present realization and investigations. *Power Systems, IEEE Transactions on*, 2(2):505 –511, may 1987.

[10] S. Archidiacono, S. Corsi, and M. Mocenigo. Studies on area voltage and reactive power at enel. *Proc. of the GIGRE, Dortmund, Germany*, 32-77-66, 1977.

[11] A.G. Phadke, J.S. Thorp, and M.G. Adamiak. A new measurement technique for tracking voltage phasors, local system frequency, and rate of change of frequency. *Power Apparatus and Systems, IEEE Transactions on*, PAS-102(5):1025 –1038, may 1983.

[12] A.G. Phadke. Synchronized phasor measurements in power systems. *Computer Applications in Power, IEEE*, 6(2):10 –15, apr 1993.

[13] A. G. Phadke, J. S. Thorp, and K. J. Karimi. State estimlatjon with phasor measurements. *Power Systems, IEEE Transactions on*, 1(1):233 –238, feb. 1986.

[14] Ashwini Chegu, Fangxing Li, and Xiaokang Xu. An overview of the analysis of cascading failures and high-order contingency events. In *Power and Energy Engineering Conference (APPEEC), 2010 Asia-Pacific*, pages 1 –5, march 2010.

[15] J S Thorp, M Ilic-Spong, and M Varghese. An optimal secondary voltage-var control technique. *Automatica*, 22(2):217–222, 1986.

[16] RA Schlueter, I Hu, MW Chang, JC Lo, and A Costi. Methods for determing proximity to voltage collapse. *IEEE Transactions on Power System*, 6(1):285–292, 1991.

[17] Stephen Boyd and Lieven Vandenberghe. *Convex Optimization*. Cambridge University Press, New York, NY, USA, 2004.

[18] P. Venkataraman. *Applied Optimization with MATLAB Programming*. Wiley Publishing, 2009.

[19] H A Eiselt and C L Sandblom. *Linear Programming and Its Applications; electronic version.* Springer, Dordrecht, 2007.

[20] Marija Ilic and John Zaborszky. *Dynamics and control of large electric power systems.* Wiley, New York, 2000.

[21] RA Schlueter, I Hu, MW Chang, JC Lo, and A Costi. Methods for determing proximity to voltage collapse. *IEEE Transactions on Power System*, 6(1):285–292, 1991.

[22] E Allen, J Lang, and M Ilic. A combined equivalenced-electric, economic, and market representation of the northeastern power coordinating council u.s. electric power system. *IEEE Transactions On Power Systems*, 23(3):896–907, 2008.

PMU Based Substation Voltage Controller

Part B

Part B Project Team

Vaithianathan "Mani" Venkaatsubramanian, Project Leader
Xing Liu, Javier Guerrero, Hong Chun, Graduate Students
Washington State University

Information about Part B

For information about Part B of this report contact:

Mani V. Venkatasubramanian
Professor, School of Electrical Engineering and Computer Science
Washington State University, Pullman, WA 99164-2752
Email: mani@eecs.wsu.edu

Power Systems Engineering Research Center

The Power Systems Engineering Research Center (PSERC) is a multi-university Center conducting research on challenges facing the electric power industry and educating the next generation of power engineers. More information about PSERC can be found at the Center's website: http://www.pserc.org.

For additional information, contact:

Power Systems Engineering Research Center
Arizona State University
527 Engineering Research Center
Tempe, Arizona 85287-5706
Phone: 480-965-1643
Fax: 480-965-0745

Notice Concerning Copyright Material

PSERC members are given permission to copy without fee all or part of this publication for internal use if appropriate attribution is given to this document as the source material. This report is available for downloading from the PSERC website.

Table of Contents

1. Task 2 Summary: PMU based substation voltage controller 1
2. PMU based voltage stability monitoring 2
   2.1 VSA Index and Its Motivation 2
   2.2 VSA Index from PMU data 4
   2.3 Example based on actual PMU data 6
3. PMU Based Substation Voltage Controller 9
4. Conclusions 13
References 14
Project Publications 16

List of Figures

Figure 1. Saddle node bifurcation example 3
Figure 2. Complementary limit induced bifurcation example 3
Figure 3. V-Q data points and the density plot for 10 seconds of PMU data 5
Figure 4. The V-Q relationship for reactive power Qij to bus voltage Vi 5
Figure 5. Points of V-Q with increasing and decreasing slopes 6
Figure 6. Time-plots of Vi and Qij for the time period from 0s to 50s 7
Figure 7. V-Q data pairs for the time period 30s-40s after Data Split 7
Figure 8. Substation local voltage controller 9
Figure 9. Overview of SLVC functions and the flowchart 10

List of Tables

Table 1. QV Line Sensitivities from PMU data after data split..... 7

1. Introduction: PMU Based Substation Voltage Controller

Coordinating the reactive power resources towards maintaining an optimal voltage profile is one of the major operational responsibilities for every power system [1], [2]. The local character of the voltage control, the diversity of the control means and the interaction among them makes this task particularly difficult. In many European countries and in China, hierarchical voltage controllers have been proposed and implemented for automatically controlling the voltage profile of the transmission network by using different notions of primary, secondary and tertiary voltage controls [3]-[10]. Pilot automatic voltage control projects have been implemented in the past at Bonneville Power Administration [11] and PJM Interconnection [12]. Much of the voltage control actions in North America are coordinated by operators by switching in or out shunt capacitor banks or reactor banks, as well as by adjusting transformer taps as needed. With large installations of synchrophasors across the North American power system and around the world, there is growing interest in developing control applications based on synchrophasors [13]. This report discusses a voltage controller for substations that mostly uses local PMU measurements.

In Section 2, a new real-time voltage stability monitor from [14] is summarized that uses local PMU measurements to derive a voltage security index. In Section 3, sensitivity results from Section 1.1 are extended towards developing a PMU based substation voltage controller.

2. PMU Based Voltage Stability Monitoring

The objective of the section is to estimate the proximity of the system operating condition to static voltage instability limit in the sense of the classical QV margin at any bus by using a few PMU measurements.

2.1 VSA Index and Its Motivation

Here Voltage Security Assessment (VSA) index Γ_i for bus i is defined as the slope of the QV curve:

$$\Gamma_i = \frac{\Delta Q_i}{\Delta V_i} = \sum_j \frac{\Delta Q_{ij}}{\Delta V_i} \qquad (1)$$

where ΔQ_{ij} represents reactive power change for each transmission line or transformer (equivalent line mode) connected with this bus. Notice that the lines are pointed to the ones in service before and after that change. ΔQ_i is an incremental change in bus injection at bus i.

The well-known fact is that power flow Jacobian becomes singular when the system is at a static saddle-node bifurcation. Hence, the slope at the critical point of Q-V curve will be infinite. Or, the VSA index Γ_i will approach zero in the sense of parameter variation of Q_i at bus i when the variation induces a saddle-node bifurcation at the nose of the QV curve.

As for the complementary limit induced bifurcation case introduced in [15], the slope $\Gamma_i = \Delta Q_i / \Delta V_i$ will likely stop at some small value instead of approaching zero when the parameter variation induces the limit induced bifurcation.

Figure 2 and Figure 3 show these two bifurcation cases in Q-V curves and the index vs. Q. Figure 1 is for bus 12 of New England 39-bus system. This is a saddle node bifurcation case. At the critical node of Q-V curve, the tangent of critical node of Q-V curve is almost vertical. Correspondingly, Γ_{12} is 1.18 which is very close to "0". Figure 3 is a complementary limit induced bifurcation case from IEEE 300-bus system. For bus 14, the power flow fails when its reactive load is approximately 470 MVAr. From Q-V curve, the slope around the critical node is apparently not infinite. This result is reflected very well on the "small" value of Γ_{14} which is 7.01 at the limit.

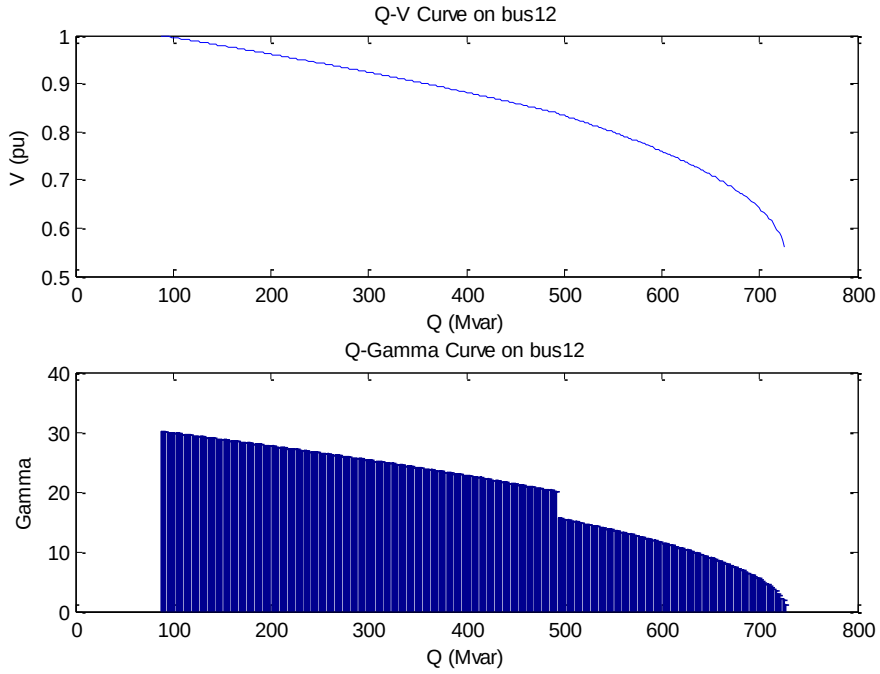

Figure 1. Saddle node bifurcation example

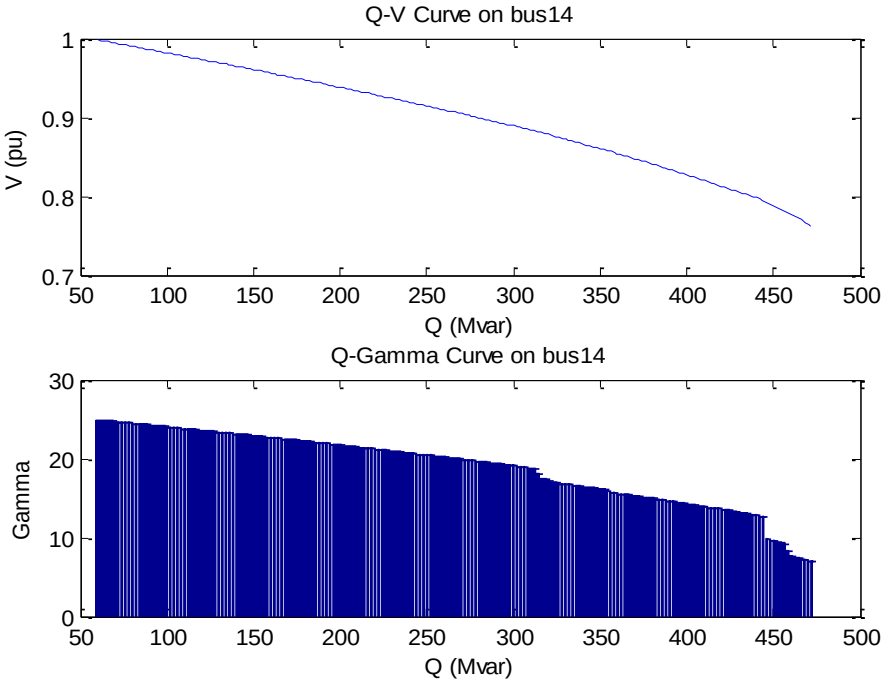

Figure 2. Complementary limit induced bifurcation example

Naturally and consequently, we conjecture the following rules only using this global index Γ_i to assess the system voltage security at any bus *i*.

The index Γ_i can assess bus voltage security by the following statements:

- ***A "high" value of Γ_i indicates a "strong" bus in terms of being distant from static voltage instability limit.***
- ***If there is any bus with Γ_i value near "0", the system is close to static voltage stability limit related to saddle-node bifucrcation, and the bus with the lowest Γ_i is likely in the critically voltage stressed part of the system.***
- ***If one system has the bus whose Γ_i is less than some critical value, say "Γ_i^*", and then the system may be vulnerable towards voltage instability caused by either of saddle-node or limit induced bifurcations. We need to pay attention to this system voltage security.***

In other words, *no matter which static bifurcation the system will encounter, the system is operating in voltage unsecure region and reactive power support needs to be corrected, if some bus has low* Γ_i. In the next section, we propose techniques for computing Γ_i from real-time PMU measurements.

2.2 VSA Index from PMU data

In this section, we plan to estimate the QV slope Γ_i from real-time PMU data by individually estimating QV line sensitivity on each of the lines connected to bus *i* and by taking the sum:

$$\Gamma_i = \frac{\Delta Q_i}{\Delta V_i} = \sum_j \frac{\Delta Q_{ij}}{\Delta V_i}$$

Philosophically, we are processing line sensitivities to detect proximity to static stability limits as in [16]. However, our approach is clearly different because we are directly extracting the QV slope Γ_i from the line sensitivities by the sum (1). The subsequent relationship of Γ_i to system static stability limit is well-defined as discussed in 2.1. Moreover, the novel contribution of this paper is the direct estimation of the line sensitivities $\Delta Q_{ij}/\Delta V_i$ from PMU data by exploiting fundamental nature of power system causality.

There have been many other recent papers (e.g., [17]) on voltage stability monitoring using PMU data which all use a combination of system model data (such as line parameters and state estimation solution) together with PMU data. Whereas our approach proposed in this paper is purely based on PMU measurement data and does not need system model information for real-time voltage stability analysis.

First, let us try to extract the slope $\Delta Q_{ij}/\Delta V_i$ for some transmission line from the sample recorded PMU data which is from an actual PMU in the eastern system. Looking at Fig 3,

a statistical fit of a linear slope on the QV data for the line shows the slope to be near zero. Even the density plot does not point to any meaningful slope $\Delta Q_{ij}/\Delta V_i$ for this line.

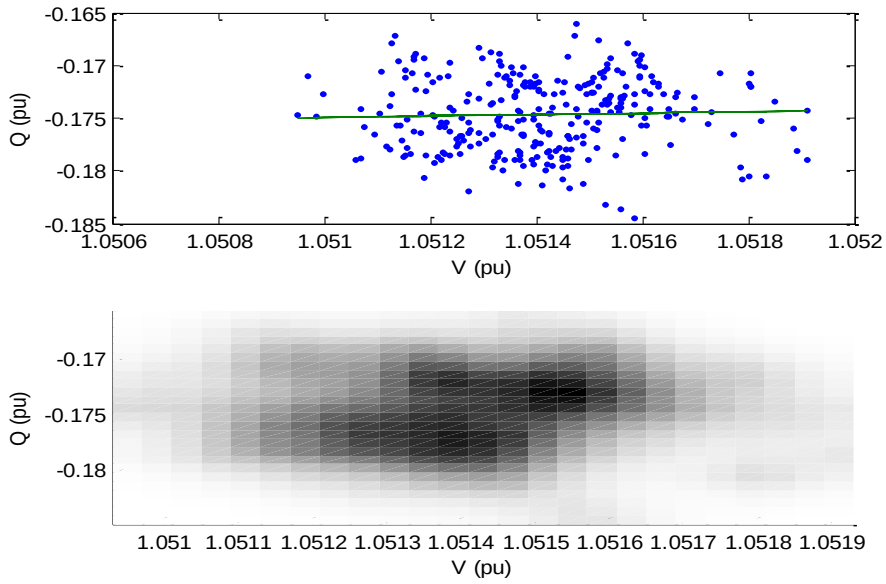

Figure 3. V-Q data points and the density plot for 10 seconds of PMU data

However, based on capacitor bank switching near the bus, we could conclude that the slope $\Delta Q_{ij}/\Delta V_i$ was definitely not zero. The apparent inconsistency why the statistical fit failed to reveal the slope could be explained by causality of Q-V relationship. In the real system, note that there are actually two slopes $\Delta Q_{ij}/\Delta V_i$ related to the transmission line from bus i to bus j. Whether the change in line-flow is affected by changes in sending end of the line or the receiving end of the line will result in two different slopes with opposite signs. Therefore, the slope can be estimated only by first dividing the data into two sets accordingly as shown next.

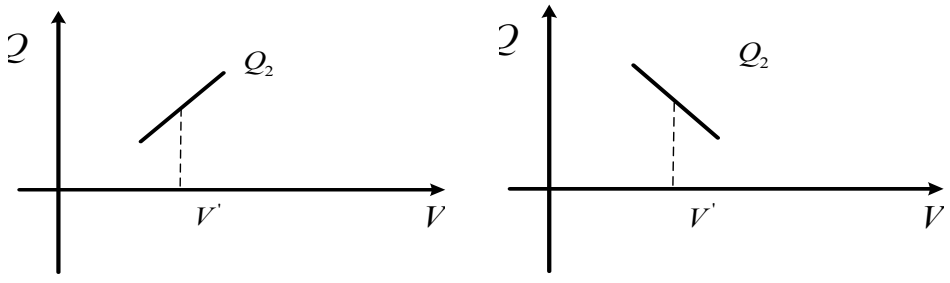

4.a Positive slope 4.b Negative slope

Figure 4. The V-Q relationship for reactive power Qij to bus voltage Vi

When the same data in Fig 3 is split according to positive slopes and negative slopes, we can clearly see the trend of the data points lining up along a definite positive slope versus a clearly defined negative slope for the sensitivity. Using statistical analysis, the two slopes can then be estimated. The slopes from these "ambient" PMU responses also match very well with sensitivities calculated from discrete switching events.

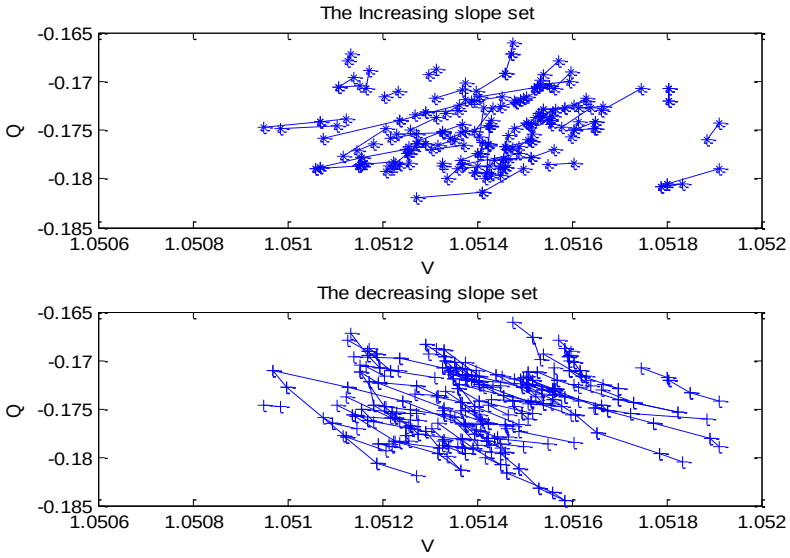

Figure 5. Points of V-Q with increasing and decreasing slopes

2.3 Example based on actual PMU data

This is a test set of PMU data where the line-flow shows a jump around 35 seconds as in Figure 6. Figure 7 shows the PMU data subsets after data split for the time-period between 30s and 40s. Table 1 summarizes the results of data analysis. In Table 1, α denotes the estimated positive slope while β denotes the corresponding negative slope for the QV sensitivity $\Delta Q_{ij}/\Delta V_i$ for this line. The value α_{Jump} is the positive slope for $\Delta Q_{ij}/\Delta V_i$ calculated directly from the discrete event near time 35 s and this value serves as a reference to crosscheck the results of statistical analysis for α and β in Table 1. We observe that the estimated slopes match well with the slope calculated from discrete jump especially for the longer span of PMU data over ten second intervals.

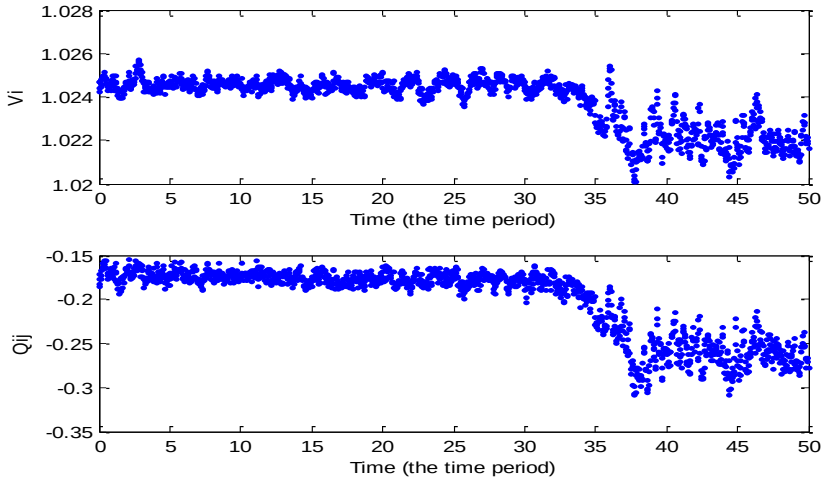

Figure 6. Time-plots of Vi and Qij for the time period from 0s to 50s

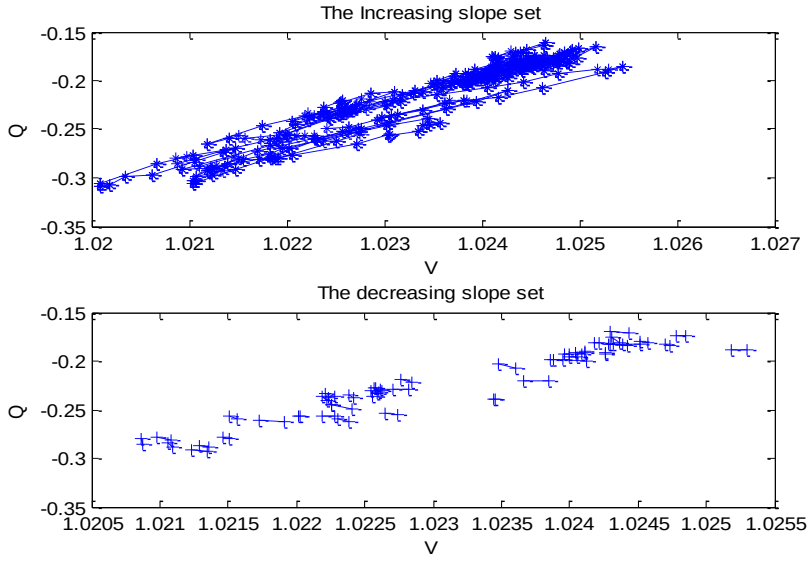

Figure 7. V-Q data pairs for the time period 30s-40s after Data Split

Table 1. QV Line Sensitivities from PMU data after data split

Sensitivity	**0s-1s**	**0s-10s**	**30s-31s**	**30s-40s**	**40s-41s**	**40s-50s**
α	38.66	38.41	49.51	41.29	28.91	36.11
β	-22.42	-28.40	-42.01	-30.36	-27.88	-40.67
α_{Jump}	42.33 around 35s					

Based on similar analysis, the line sensitivities $\Delta Q_{ij}/\Delta V_i$ can be calculated for each of the lines connected to bus i giving us the net sum Γ_i in (1) which is then the VSA index for bus i. Whenever the value Γ_i goes below a predefined threshold, say "$\Gamma_i^* = 10$", the system near the monitored bus is approaching static voltage stability limit as discussed earlier in Section 2.1.

Details on the statistical analysis as well as simulation results on test systems will be presented elsewhere. The algorithms have also been implemented into openPDC platform in a prototype fashion at Tennessee Valley Authority (TVA), and the results will be presented elsewhere.

3. PMU Based Substation Voltage Controller

The objective of this section is to propose a Substation Local Voltage Controller (SLVC) that uses mostly local PMU measurements for controlling the local VAR devices at the substation, namely, tap-changing transformers, shunt capacitor banks, shunt reactor banks, and series capacitor banks. The formulation assumes that the bus voltage references or schedules for the substation are specified by a higher level central coordinator [18]. The aim of the local substation controller is to manage discrete VAR resources at the substation to maintain the local bus voltages at the specified voltage schedules.

The benefits of the substation controller are as follows:

1) Automation of the switching operations thus reducing the burden on substation operators.
2) Efficient voltage regulation of different voltage levels while minimizing the number of switching actions. Reducing the number of tap changer operations enhances the longevity of the banks while also reducing maintenance costs.
3) Monitoring and eliminating circular VAR flows among multiple parallel transformer banks at the substation. Circular VAR flows if left uncorrected lead to unnecessary flow of reactive power back and forth among parallel transformers leading to increased heating losses while also depleting valuable VAR resources.
4) Early detection of unusual operating conditions related to highly stressed system scenarios that are seen from significantly different system responses after routine switching events.

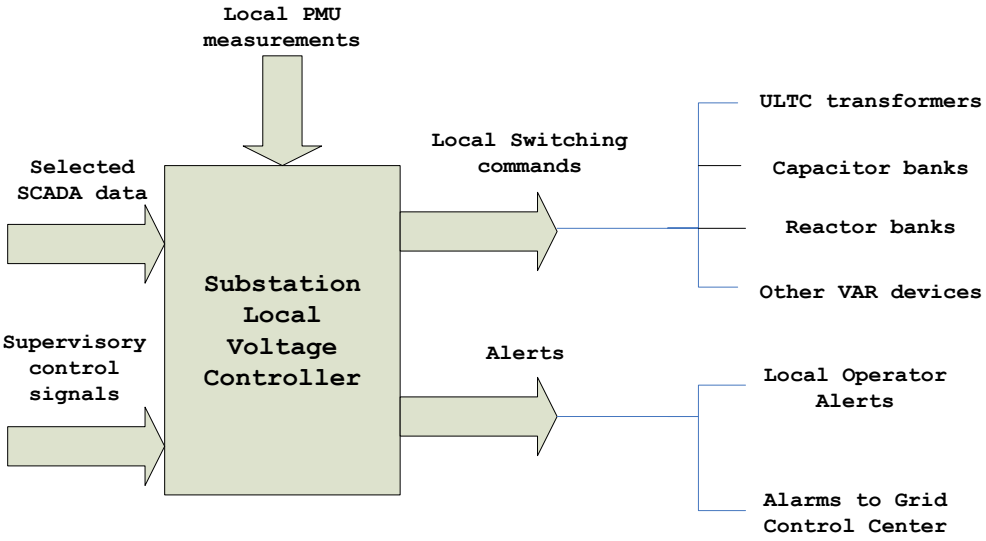

Figure 8. Substation local voltage controller

In general, the substation controller as proposed will need to work hand-in-hand with other local voltage controls such as generator Automatic Voltage Regulator (AVR) and

Static VAR Compensator (SVC). For sake of illustration, we will assume that there is also an SVC at the substation of interest that regulates say the 500 kV bus voltage. For illustration, we assume that the Substation voltage controller will maintain other voltages at the substation, say the 230 kV and 115 kV bus voltages. It is suggested that the controller operate in two operating modes depending on whether SVC is in service or not.

SLVC Slave mode: When SVC is in service, the SLVC controller will operate in Slave mode. In this mode, SLVC will monitor and control all available discrete devices while primarily maintaining voltage schedules at 230 kV and 115 kV buses while also keeping SVC VAR output near zero as a secondary control objective. Methodology of mathematical formulation of the Slave mode is presented in Section 3.1.

SLVC Master mode: When SVC is not in service, SLVC will take over maintaining voltage schedules of 230 kV and 115 kV and 500 kV bus by controlling all available discrete control devices at the substation. Formulation of Master mode will be discussed in Section 3.2.

The overall framework of SLVC is summarized in Figure 9.

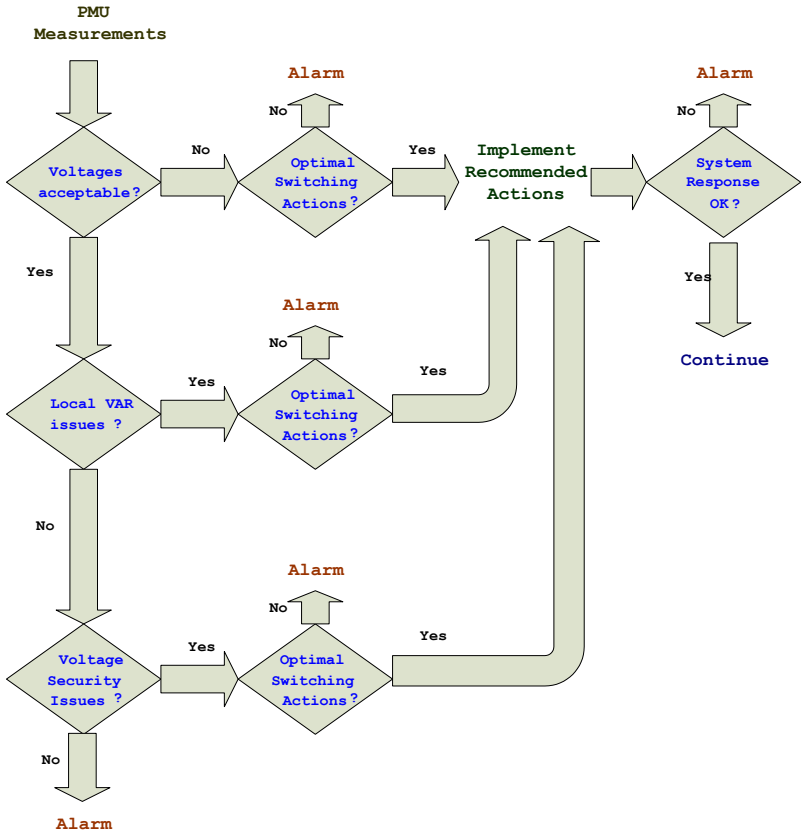

Figure 9. Overview of SLVC functions and the flowchart

The primary responsibility of SLVC is to maintain the substation bus voltages close to specified voltage schedules. When all voltages are within acceptable tolerances, the controller will look into local VAR issues such as elimination of local circular VAR flows, maintenance of adequate VAR reserves at local SVC device as well as from local shunt VAR devices. An optional functionality is also the ability to issue voltage insecurity alerts or alarms using algorithms previously discussed in Section 2.

3.1 SLVC Slave Mode Formulation

SLVC is proposed as a discrete controller that will choose an optimal switching action among all feasible control actions for that control iteration. In this mode, SLVC assumes that SVC is in charge of keeping the 500 kV voltage at near the specified value. Accordingly, SLVC will only monitor and maintain 115 kV and 230 kV voltages.

The controller objectives and priorities are assumed to be:

1) Maintain 115 kV bus voltage within specified range
2) Maintain 230 kV bus voltage within specified range (determined by hierarchical central optimization process [18])
3) Monitor and eliminate circular VAR flows if any exist
4) Keep SVC VAR output within specified range

Step 0: (Design): Formulate the set of possible control actions: a) switching of 500 kV capacitor and reactor banks, b) switching of 230 kV capacitor and reactor banks, c) switching of 115 kV capacitor and reactor banks, e) switching of 500 kV-230 kV transformer banks LTC, f) switching of 230 kV-115 kV transformer banks LTC. The control actions will mostly consist of single discrete actions such as switching in or out of a capacitor bank. Some of the actions can also be "multiple switching" such as: simultaneous switching of parallel transformer banks LTC's, or changing of multiple taps, or switching of parallel capacitor banks as needed. Basically SLVC design will facilitate the design engineers to pre-specify the set of possible control actions as part of the design formulation.

Step 1: (Approach) Control formulation assumes that SLVC can predict (in real-time) the post switching voltage levels and VAR flows on transmission lines connected to the substation for each of the control actions specified by the user in Step 0. As summarized in Section 2, we have developed novel techniques for carrying out such local reactive power-voltage calculations based on real-time QV sensitivities of local PMU measurements. As a back-up measure, we can keep a record of sensitivities of VAR flows and voltages as related to recent control actions (say average effect from the latest two or three switching actions) by continuous monitoring of PMU values. In each control iteration, these sensitivities will be used to identify feasible controls and to rank them.

Controller iteration: (Real-time algorithm) Controller is proposed as a simple logical controller that chooses best feasible control action among a user-specified set of candidate control actions by pre-specified design rules:

a) Check for violation of any of the controller objectives 1 through 4 above. If none, wait for next iteration.

b) If in violation, compute post-switching values of bus voltage and VAR flows using sensitivities of step 1 above for each of the candidate control actions in Step 0. Identify feasible control actions that meet all objectives 1 through 4. If no feasible control actions meet all of objectives 1 through 4, identify those action that meet objectives 1 through 3. If none exist again, find those controls that meet objectives 1 and 2. If none exist, notify the operator that no control actions found. (Or we can relax objective 2 as well and try to meet objective 1 alone on maintaining 115 kV voltage).

c) From feasible control actions of b), eliminate those devices which were switched in the recent past (to eliminate those actions which are not possible from device limitations). We will maintain the last switching time as well as number of switching actions for each of the control actions in step 0 with specified limitations.

d) Rank eligible control actions for suitability to control objectives. Switching out actions will be ranked higher than controls that switch in a device. Switching of shunt/reactor banks may be preferred over tap changes. After these two rules, actions that reduce the circular VAR flows and that reduce SVC VAR output will be ranked higher.

e) Implement highest ranked control action from d). Update switching history of that control action.

f) Verify whether the post-switching values are within acceptable range of predicted post-switching values of b). If actual post-switching values are substantially different, notify the SLVC engineering support and issue alarm to the operator to watch over SLVC.

g) Move to next control iteration with possibly 1 second or two seconds between control iterations.

3.2 SLVC Master Mode Formulation:

The controller objectives and priorities are assumed to be:

1) Maintain 115 kV bus voltage within specified range
2) Maintain 230 kV bus voltage within specified range (determined by hierarchical central optimization process [18])
3) Maintain 500 kV bus voltage within specified range (determined by hierarchical central optimization process [18])
4) Monitor and eliminate circular VAR flows if any exist

Rest of the formulation and controller algorithm is very much like in the Slave mode. Control iteration time may also be made shorter for this mode. Otherwise the algorithm will work exactly as in Slave mode formulation.

4. Conclusions

The report proposes a PMU based substation voltage controller. Novel algorithms for direct estimation of QV line sensitivities from real-time streaming PMU data are proposed first in Section 2. The algorithms are shown to be effective in detecting voltage insecurity scenarios in the power system. Voltage Security Index proposed at each bus is useful to classify voltage strong buses versus voltage weak buses in terms of reactive power support at the bus. In Section 4, initial formulation of a substation voltage controller is proposed. The controller uses QV sensitivity values from Section 2 to carry out local power-flow like calculations to predict expected bus voltage levels after discrete switching actions. The substation controller then coordinates the switching of local VAR devices to manage the discrete VAR devices at the substation towards maintaining voltage schedules for different voltage levels at the substation. Future research is indicated on two-level control formulations that may include central higher-level coordinator and many local substation controllers such as discussed in [18].

References

[1] P. Kundur, *Power System Stability and Control*, McGraw-Hill Inc., 1994.

[2] C. W. Taylor, *Power System Voltage Stability*, McGraw-Hill Inc., 1994.

[3] J.P. Paul, J.T. Leost, and J.M. Tesseron, "Survey of the Secondary Voltage Control in France: Present Realization and Investigations," *IEEE Transactions on Power Systems*, Vol. PWRS-2, No.2, pp. 505-511, 1987.

[4] R. Yohoyama, T. Niimura, and Y. Nakanishi, "A Coordinated Control of Voltage and Reactive Power by Heuristic Modeling and Approximate Reasoning", *IEEE Transactions on Power Systems*, Vol. 8, No. 2, pp. 636-645, May 1993.

[5] M. Ilic, J. Christensen, and K.L. Eichorn, "Secondary Voltage Control Using Pilot Point Information", *IEEE Transactions on Power Systems*, Vol. 3, No. 2, May 1988.

[6] S. Corsi, P. Marannino, N. Losignore, G Moreschini, and G. Piccini, "Coordination Between the Reactive Power Scheduling Function and the Hierarchical Voltage Control of the EHV ENEL System", *IEEE Transactions on Power Systems*, Vol. 10, No. 2, pp. 686-694, May 1995.

[7] J. L. Sancha, J. L. Fernandez, A. Cortes, and J. T. Abarca, "Secondary Voltage Control: Analysis, Solutions and Simulation Results for Spanish Transmission System", *IEEE Transactions on Power Systems*, Vol. 11, No. 2, May 1996.

[8] H. Vu, P. Pruvot, C. Launay, and Y. Harmand, "An Improved Voltage Control on Large Scale Power System", *IEEE Transactions on Power Systems*, Vol. 11, No. 3, August 1996.

[9] J. Van Hecke, N. Janssens, J. Deuse, and F. Promel, "Coordinated Voltage Control Experience in Belgium", *CIGRE Session Report 38-111*, Paris, September 2000.

[10] H. Sun, Q. Guo, B. Zhang, W. Wu, and J. Tong, "Development and applications of system-wide voltage control system in China", Proc. IEEE PES General Meeting, 2009.

[11] K.Tomsovic, D.E.Bakken, V.Venkatasubramanian, and A. Bose, "Designing the next generation of real-time control, communications and computations for large power systems", *Proceedings of the IEEE*, vol. 93, no. 5, May 2005.

[12] J.Tong, D.W.Souder, C. Pilong, M.Zhang, Q. Guo, H. Sun and B. Zhang, "Voltage control practices and tools used for system control of PJM", *Proc. IEEE PES General Meeting,* 2011.

[13] C.W. Taylor, D. Erickson, K. Martin, R. Wilson, V. Venkatasubramanian, "WACS – Wide-area stability and voltage control system: R&D and online demonstration," *Proceedings of the IEEE*, vol. 93, no. 5, May 2005.

[14] X. Liu, G. Liu, M. Sherwood, and V. Venkatasubramanian, "Wide-Area Monitoring and Control Algorithms for Large Power Systems using Synchrophasors", Proc. IREP International Symposium on Bulk Power System Dynamics and Control, Brazil, August 2010.

[15] X.Yue and V. Venkatasubramanian, "Complementary Limit Induced Bifurcation Theorem and Analysis of Q limits in Power-Flow Studies", *Bulk Power System Dynamics and Control-VII. Revitalizing Operational Reliability, 2007 iREP Symposium*, pp. 1-8, 19-24 Aug. 2007.

[16] B. C. Raczkowski and P. W. Sauer, “Identification of Critical Cutsets for Static Collapse Analysis", *Bulk Power System Dynamics and Control-VII, Revitalizing Operational Reliability, 2007 IREP Symposium*, pp. 1-8, 19-24 Aug, 2007.
[17] M. Glavic and T. Van Cutsem, “Detecting with PMUs the onset of voltage instability caused by a large disturbance”, Proc. IEEE PES General Meeting, July 2008.
[18] V. Venkatasubramanian, H. Chun, J. Guerrero, F.Habibi-Ashrafi, and A. Salazar, “Hierarchical two-level voltage controller for Southern California Edison”, *Proc. IEEE PES General Meeting*, 2012, to appear.

Project Publications

[1] X. Liu, G. Liu, M. Sherwood, and V. Venkatasubramanian, "Wide-Area Monitoring and Control Algorithms for Large Power Systems using Synchrophasors", *Proc. IREP International Symposium on Bulk Power System Dynamics and Control*, Brazil, August 2010.

[2] V. Venkatasubramanian, H. Chun, J. Guerrero, F.Habibi-Ashrafi, and A. Salazar, "Hierarchical two-level voltage controller for Southern California Edison", *Proc. IEEE PES General Meeting*, 2012, to appear.

Identifying External Network Branch Status Errors Using Synchronized Phasor Measurements

Part C

Part C Project Team

Ali Abur, Project Leader
Roozbeh Emami, Graduate Student
Northeastern University

Information about Part C

For information about Part C of this report contact:

Ali Abur
Professor
Department of Electrical and Computer Engineering
Northeastern University
315 Huntington Ave.
Boston, MA, 02115
abur@ece.neu.edu

Power Systems Engineering Research Center

The Power Systems Engineering Research Center (PSERC) is a multi-university Center conducting research on challenges facing the electric power industry and educating the next generation of power engineers. More information about PSERC can be found at the Center's website: http://www.pserc.org.

For additional information, contact:

Power Systems Engineering Research Center
Arizona State University
527 Engineering Research Center
Tempe, Arizona 85287-5706
Phone: 480-965-1643
Fax: 480-965-0745

Notice Concerning Copyright Material

PSERC members are given permission to copy without fee all or part of this publication for internal use if appropriate attribution is given to this document as the source material. This report is available for downloading from the PSERC website.

Table of Contents

1. Introduction 1
1.1 Background 1
2. Overview of the Problem 3
2.1 Linear Formulation 7
2.2 Nonlinear Formulation 10
3. Simulation Results 13
3.1. Linear Formulation 13
3.2. Nonlinear Formulation 16
4. Conclussions 20
References 21
Project Publications 23

List of Figures

Figure 1 Schematic of inter connected system 4
Figure 2 *B* matrix for a given system 5
Figure 3 Simulation of a line outage with active power injection 5
Figure 4 Change in *B* due to removal of the line *l*. 6
Figure 5 Typical B_{12} for a given system. 12
Figure 6 Internal and external system boundaries in IEEE 118 bus system 15
Figure 7 IEEE 30 bus system split into two sub-systems 17

List of Tables

Table 1. Test result for 118 bus system 15

Table 2. Results for 118 bus system with 2% change in load/generation..... 16

Table 3. Test result for 30 Bus system, line outage with constant operating condition
..... 18

Table 4. Test results for 118 bus system using power flow solutions 18

Table 5. Test result for IEEE 30 Bus system, line outage with 2% change in operating condition
..... 19

Table 6. Test result for IEEE 118 Bus system, line outage with 2% change in operating condition
..... 19

1. Introduction

1.1 Background

Static security assessment for a power system involves real-time contingency analysis, which requires an accurate network equivalent to be maintained and used to represent the external system. The results of contingency analysis will determine whether or not further corrective actions have to be taken in order to ensure that the system remains in the normal and secure operating state. Any errors in the contingency analysis will therefore lead to incorrect decisions with regards to the current and forecasted operating state of the system.

Topology of the system is determined based on the telemetered status of circuit breakers and switches. The dynamic data such as analog and digital measurements along with static data like branch parameters are used in network configuration and state estimator to estimate the real-time condition of the network.

If a switch or circuit breaker is part of the model, but it is not remotely monitored, its open or close status may be incorrectly reported. Such situations will lead to topology errors for all the application functions that rely on the system model provided by the topology processor. Topology errors associated with branches in the external system are even harder to detect and identify due to the limited number of real-time measurements received from the external system.

Utilizing synchronized measurement devices such as phasor measurement units (PMUs) can potentially help to alleviate such problems, improve chances of identifying external line outages and subsequently increase the accuracy of the overall static security analysis.

So far, several methods to detect and identify measurement [1-4] and topology errors [5-13] have been proposed and documented in the literature. Others have investigated the problem of detecting branch outages in external systems [14-15]. Recent report on the Blackout of 2003 emphasizes the importance of having the connectivity information about the external system in order to avoid such system failures [16]. Using redundant measurements and the state estimator, breaker status can be estimated as a way to track network topology, provided that such redundancy exists in the available real-time measurements [17-18].

This report proposes an optimization based alternative to track changes in the status of external system branches. The presented approach uses internal system bus phase angles

for both pre-outage, and post-outage stages, as well as the base case topology of the system to identify the external line outage. If available, it incorporates the information from phasor measurements taken from substations in the external system, in order to further improve the topology tracking capability.

Given the fact that system operating conditions change continuously, it is necessary to differentiate between changes due to normal load variations and branch outages. The proposed method is designed to make this differentiation.

Redundancy of measurements and accurate knowledge of network topology are critical factors in estimation of the system state. It is noted that in any inter-connected system, the internal system plus boundary buses constitute an observable island based on the internal system measurements. Hence, those measurements used for the external system, are either pseudo-measurements provided by the load forecasting and/or generator scheduler functions or they may seldom contain actual real-time measurements received through inter-utility real-time measurement exchange.

In either case, due to lack of redundancy, their impact on the internal state estimation will be minimal or null. Since external topology follows the same rule, its impact on internal state estimation is minimal. On the other hand, they may have a significant impact on contingency analysis associated with internal system topology changes; also identified as one of the major reasons in previous black outs in North America [19]. Since the load and generation changes are gradual, assuming that the measurement scan take place often enough, shift in load or generation usually do not have a critical impact on internal contingency analysis. On the other hand, external topology error may have crucial impact on internal security analysis.

The U.S electric transmission network is an interconnected network where an outage in one state can cause cascading blackouts in other states or neighboring countries [20]. Most of the utility companies in United States have a few PMUs available in their systems whose phasor measurements are available to the internal power system dispatcher in real-time. Therefore it is worth investigating the incremental benefits to be gained by taking advantage of their limited presence in the system. One such advantage would be external topology error detection using real-time internal data along with a few real-time data available through external PMUs which can in turn, help improve the internal security analysis.

It is well documented that knowledge of internal system about the connectivity information of the external system in an inter-connected network is very important for the system operation [16].

This report proposes a new method to identify the external line outage. For simplicity, and illustration, the linear decoupled model of the power system can be used to develop power system model, and extract the formulation. Extracted formulation can be tested

using the synthetic dc data, obtained through calculation, and then the formulation will be modified in such a way that it can be used for the case of using real power flow solutions as well. The presented method in this report is one possible method which uses the local internal phase angles and those phase angles available from external PMUs for both base-case (pre-outage), and post-outage stages, as well as the base-case topology of the system to identify the external line outage.

The report is organized as follows: Section 2 describes the problem overview. Section 2.1 formulates the problem for the case where DC power flow solution is used. Section 2.2 shows the required change in formulation in order to handle the actual AC power flow solution. This is followed by an integer programming problem whose solution identifies the external line outage in section 3. The validation example is represented in this section, where, IEEE 118 bus system as well as IEEE 30 bus system are divided into two sub-systems, representing internal and external systems, and different line outages are simulated in the external system to validate the proposed method.

2. Overview of the Problem

The problem addressed in this report is identification of the external topology change, using the real-time internal state and internal measurements as well as the real-time phasor measurements through external PMUs. The proposed method utilizes the decoupled linear model of power systems to simulate the network. For simplicity, the method is initially used to identify the external line outage using error-free DC data, and then the formulation will be adjusted in such a way that it solves the real power flow solution case as well.

Accurate power system operation requires close monitoring of system topology and measurements. In a given inter-connected power system such as the one shown in figure 1, the internal system is defined as the part of the system which is under study, and the part external to the boundaries of internal system, is defined as the external system. Real-time information about internal measurements and internal topology is available to internal power system dispatcher whereas, very limited information about external measurements and external topology is available to the internal power system operator.

Inter-utility real-time data exchange became a very important application in interconnected systems during past a few decades. Real-time and historical information of any system in wide area networks will be sent to inter-control center, to be used by external systems. (Inter-control Center Communication Protocol) ICCP allows the real-time and historical exchange of information such as circuit breakers status, measurement

data, scheduling data, energy accounting data, and operator messages [21]. Although, each system has a limited access to external system information through ICC, usually this information is not enough to accurately model the external system prior to executing the security analysis for a given system.

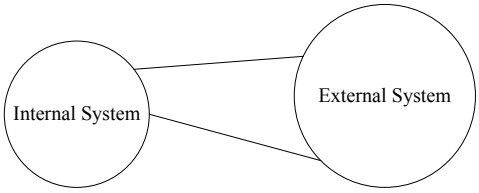

Figure 1. Schematic of inter connected system

Assuming that each subsystem along with its measurements constitutes an observable island, the state of the system can be estimated without having access to any external network measurements or external network topology. On the other hand, execution of the real-time contingency analysis function for the internal system requires the use of an equivalent of the attached external systems. Therefore, inaccuracy in external topology or load/generation may have significant impact on the outcome of internal system contingency analysis.

Although the external network operating conditions also influence the results of internal security analysis, their impact on internal contingency analysis is relatively small due to the fact that the load/generation of a system usually does not change drastically in a short period of time. On the other hand, even a single line outage in the external system may have significant impact on security analysis of the system. Therefore tracking topology changes in the external system is critical for the internal system operator. Since it is currently impossible to have real-time access to all circuit breakers status through ICCP, an approach to identify external line outages based on internal topology and measurements as well as a few real-time external phasor measurements will be very useful in topology tracking.

The problem of topology change identification is initially formulated using the linear decoupled power system model. The formulated problem is solved using an optimization method which will be explained in detail below. The proposed solution method is then tested using simulated measurements obtained using the linear (DC) system model. This formulation will be subsequently revised to account for the more realistic non-linear (AC) system model.

The decoupled power flow model is well defined in [19].

$$J_{11}\Delta\theta = \Delta P(x)$$
$$J_{22}\Delta|V| = \Delta Q(x) \qquad (1)$$

where J_{11} and J_{22} are block diagonal entries of the Jacobian. Using the flat voltage profile, (1) can be written as follows:

$$B\Delta\theta = \Delta P \qquad (2)$$

where $\Delta\theta$ is change in bus angles due to change in ΔP. *B* matrix can be determined using the line status and network parameters. For a given system, *B* matrix can be formed as follows:

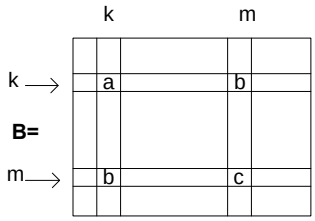

Figure 2. *B* matrix for a given system

where *b* is the susceptance of the line connecting bus *k* to bus *m*. *a*, and *c* are sum of susceptances of all branches incident to bus *k* and *m* respectively.

In linear decoupled power flow method, effect of a given line outage (*l*) can be represented by two power injections at both ends of the removed line.

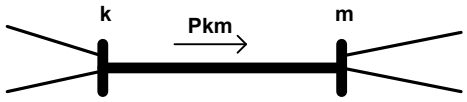

(a)

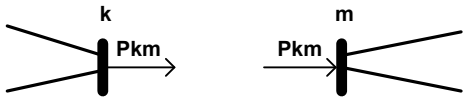

(b)

Figure 3. Simulation of a line outage with active power injection

Therefore, any line outages in the system can be represented as two power injections at ends of the removed line. Also, imposing a change in power injection will lead into alteration in phase angles of the system (2). Since the internal phase angles are always

available to the internal power system dispatcher, the objective of the proposed method is to track the change in internal phase angles and find the corresponding external power injections which may cause such shift in internal phase angles.

Let line *l*, connecting bus *k* to bus *m* in the system with *B* matrix (as shown in figure 2), be removed. Since the topology of the system is changed, new *B* matrix can be defined for post outage system (B_1). B_1 is related to pre-outage *B* matrix through following equation:

$$B_1 = B + \Delta B \tag{3}$$

Where ΔB represents the change in topology of the system and is a matrix with the same size as *B*, whose entries are all zero except for four entries corresponding to bus *k* , and *m* as shown in figure 4 [22]. Therefore:

$$\begin{aligned} B\theta_0 &= P_0 \\ B\theta_1 &= P_0 - \Delta P \\ (B + \Delta B)\theta_1 &= P_0 \end{aligned} \tag{4}$$

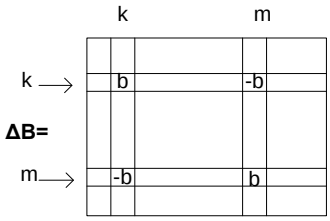

Figure 4. Change in *B* due to removal of the line *l*.

where θ_1 is the new angle solution after the line outage. Note that, even though bus injections P_0 remain the same (see the last equation in (4)), the same angle solution θ_1 can be obtained by assuming fixed topology but an equivalent change in injection vector ΔP (middle equation in (4)).

$$\Rightarrow \Delta B\theta_1 = \Delta P \tag{5}$$

where:

$$\Delta P = [0 \dots p\ 0 \dots . -p\ 0 \dots 0]^T \tag{6}$$

and *p* is the pre-outage flow on the removed line (*l*); which can be written in following form

$$p = b(\theta_k - \theta_m)$$

The presented method in this report is developed based on the assumption that internal power system dispatcher has access to real-time and historical internal line status, internal MW, and MVAR, as well as base-case external measurements and line status. Having access to the base case external topology and measurements, any internal security analysis can be accurately implemented as long as the external topology and external operating condition remains in the same condition. Any un-reported change in external topology, may lead to crucial errors in internal contingency analysis.

In case of un-reported line outage, the internal power system operator assumes that un-reported line outage is still in place, and therefore the base case equivalent will be used. In case of a change in external topology, the external network equivalent will be no longer valid, and therefore outcome of the subsequent security analysis would be in error.

The topology of the system may change due to planned outages, and seasonal load changes, or due to events such as storms, hurricanes, or lightning strikes. Also, real-time access to the status of all external circuit breaker is currently not fully available; therefore, a method which can identify external line outages (especially major line outages) will help utilities to improve their security assessment.

2.1. Linear Formulation

Assuming that enough measurements are available to make the internal system fully observable, real time internal state can be estimated. Hence, real-time phase angles of internal system will always be assumed to be known in this study. Also, it will be assumed that base case external topology and power injections are available while no knowledge about real-time external system phase angles except for those buses with PMUs will be assumed. Therefore, equation (2) can be partitioned into two parts:

$$\begin{pmatrix} \Delta P_1 \\ \Delta P_2 \end{pmatrix} = \begin{pmatrix} B_{11} & B_{12} \\ B_{21} & B_{22} \end{pmatrix} \begin{pmatrix} \Delta\theta_1 \\ \Delta\theta_2 \end{pmatrix} + \begin{pmatrix} e_1 \\ e_2 \end{pmatrix} \qquad (7)$$

Top equation is corresponding to the internal system and is identified by index 1, and the bottom part represents the external system in linear decoupled equation and is identified by index 2. As shown in previous section, any change in topology can be modeled with a pair of injections at terminals of the removed line while pre-outage topology in use. With fixed B matrix, Right hand-side of equation (7), and subsequently $\Delta\theta_1$ and $\Delta\theta_2$ would be always zero unless a change happens in load/generation of the

system. As mentioned, real-time access to the external circuit breaker status is not currently possible. Equation (4) through (6) shows that any change in topology of the system can be represented as two power injections at ends of the removed line if the system topology is kept in its base case. This can be formulated as equation (7). Therefore, application of equation (7) can help us to find two ends of the removed line.

Elimination $\Delta\theta_2$ form (7), yields:

$$J = M\Delta P_2 - e \qquad (8)$$

where :

$$(B_{12}B_{22}^{-1}B_{21} - B_{11})\Delta\theta_1 + \Delta P_1 = J$$

$$B_{12}B_{22}^{-1} = M$$

$$e = e_1 - B_{12}B_{22}^{-1}e_2$$

Any change in external topology causes shift in internal phase angle. Since the *B* matrix is assumed to be constant, equation (8) blames ΔP_2 for any change in θ_1. A single external line outage with constant operating condition can be modeled with the pre-outage topology plus two injections at terminals of the removed line (equation (4) through (6)).

Let's assume that external line *(l)* connecting bus *k* to bus *m* with pre-outage load flow *(p)* is taken out. Line outage can be simulated with imposing appropriate injections (*p* and –*p*) at bus *m* and *k*, to the pre-outage system. This can be written as:

$$\begin{matrix} & 1 & 2 & \dots & m & \dots & \dots & k & \dots & n \end{matrix}$$

$$\Delta P_2 = (0 \quad 0 \quad \dots \quad p \quad 0 \dots \quad -p \quad 0 \dots 0)^T \qquad (9)$$

Since the topology is assumed to be constant, and due to having access to both real-time and historical information of internal system, the left hand-side of equation (8), as well as the first two terms of right hand side of (8), are always known to internal power system operator.

For a system with *N* internal buses and *M* external buses, *J* is an *N* by 1 vector, and γ is an *N* by *M* matrix. ΔP_2 is an unknown vector with zero entries for all external buses except for those corresponding to the ends of the removed line. Using (9), (10) can be written as:

$$J = Mp\begin{bmatrix} 0 \\ . \\ . \\ +1 \\ 0 \\ . \\ . \\ -1 \\ 0 \end{bmatrix} + e = MpT + e \qquad (10)$$

Where T is an M by 1 vector and non-zero entries of T identify both ends of the removed line, and p is pre-outage load flow of the external line outage.

Equation (10) is a non-linear mixed integer programming where both location and values of injections are unknown. This equation should be fed into an integer programming package to be solved. One way to solve (10) is to define new matrices so that ΔP_2 can be represented as multiplication of a floating point by a binary vector. Appropriate matrices can be defined as follows:

$$M = \Lambda p(0 \ldots .1 \ 0 \ldots 1 \ 0..0)^T = \Lambda pX \qquad (11)$$

Where $\Lambda = [M \quad -M]$, and X is a binary vector of length *2Mx1*. Equation (11) can be formulated as follows:

$$\begin{cases} \min(\sum|e_{2_i}|) \\ s.t. \quad J = \Lambda.p.X + e \\ \sum_i X_i = 2 \end{cases} \qquad (12)$$

Where x_i is the *i*th entry of vector X. solutions of (12), yields location and pre-outage load flow of the removed line in external system. Applying (12) to any single line outage in external system with constant operating condition, yields two non-zero entries, the one in the first half of X vector represents the '*to-bus'* end of the line, and non-zero entry in second half of X, represents the *'from-bus'* end of the removed line.

While equation (12) can identify the line outage when real power flow solution is used or when both topology and operating condition change in error free data, it can be written in simpler way to handle the case of a single line outage when error free data in use.

Using the linear decoupled model to represent the power system is an approximation. Like any other approximation, this model introduces error when real power flow solution

is in use. On the other hand, the error term in equation (8) should be dropped, when working with error free data. This will cause slight change to equation (8) before it can be used for the error free case; otherwise the objective of equation (12) (minimizing lumped error) will be always satisfied irrelevant of the choice of buses identified as two ends of the removed line.

2.2. Nonlinear Formulation

Section 2.1, investigates the identification of external line outage, using the linear decoupled model, and calculated state and power injections of the system. Since the calculation is used, the obtained result is accurate enough that the IP package can identify ends of the removed line without need of any additional information from external system. Generally there are two approximations that are hidden in the proposed method. These approximations are the source of error in case of using real power flow solution for a system (ac case). The first source of error, is the power miss match in the transmission line: While in the DC case, any line outage can be modeled with adding and subtracting the pre-outage load flow of the line to terminals of the removed line, in the ac case, the injection values is slightly different due to power loss on transmission line.

Second term of error is induced to the formulation due to using of linear decoupled method to model the power system. Therefore equation (12) should be adjusted in case of using real power flow solutions.

Based on above explanation equation (12) is ignoring two facts that can be represented as source of errors: first one is the error term due to usage of linear decoupled method to represent the system. This error is applied to all system since it corresponds to the modeling of the system; the other is the term of error representing the power loss due to power transfer from one end of the line to another. This error is only applied to buses located ay ends of the removed line. Thus equation (12) for the ac case can be written as follows:

$$\begin{cases} \rho = \min(\sum |e_{2_i}|) \\ s.t. \quad J = \Lambda.p.A + \Lambda.q.C + \mathrm{e} \\ \quad \sum_i A_i = 2 \\ \quad \sum_i B_i = 1 \\ \quad \forall \mathrm{i},\ A_i \geq B_i \\ \quad \forall \mathrm{i},\ |e_{2i}| < \left|\frac{p}{10}\right| \end{cases} \tag{13}$$

Where Λ, and J are matrices define in section 2, p, and q are positive floating points, A is a binary vector with two non-zero entries, representing two ends of the removed line, C is a binary vector with one non-zero entry and non-zero entry in C represents the power difference between the two ends of the removed line, in other words it represents the end of removed line whose active power is less than the other one due to power loss. e is a vector corresponding to the error produced due to the approximation of the power system with the linear decoupled model. e_{2_i} is the i^{th} entry of vector e_2.

The first set of constraints in (13) guarantees the validity of (8) for the calculated results. The second set of constraints means that the binary vector A needs to have only two non-zeros indicating two ends of the removed line. The third constraint about binary vector C allows C to only have one non-zero entry. Fourth constraint makes sure that the location of non-zero entry in C is consistent with the location of one of the non-zero entries in A. This is necessary due to the power difference between two ends of the line in AC case. The last constraint makes sure that the power injections at terminals of the removed line are larger that error entries. This constraint is especially helpful in case of change in operating condition with the constant topology. Removing of this constraint from the equation set will lead to wrong solution in case of load/generation change with constant topology in external system. In such condition, having the last constraint dropped in equation (13) will cause the IP package to detect a minor external line outage plus an error vector. This happens while no topology change is occurred in actual system.

As mentioned earlier, in order for (12) to be solved for the ac case, additional constraints should be introduced to this equation (equation (13)). Although these changes seem to be necessary to solve the problem, using the real power flow solution, may not be enough to make the problem solved due to excessive available error. In other words, the error due to the model approximation and power loss on removed transmission line may cause multiple solutions for some line outages especially if pre-outage power flow of the remove line is not large enough to dominate both of the errors. Therefore, assist of a device which can provide real-time data from external system is required for solving the problem. Phasor Measurement Units (PMUs) is one of the best candidates, which can provide real-time information about external system.

PMUs are rapidly populating the power systems due to their ability of directly measuring the state of the power system, as well as other advantageous such as providing synchronized measurements, and speed and accuracy of measurements. Most of the power system utilities have a few PMUs already installed in their systems. Utilizing these available external measurements will help to overcome the problem of multi-solution for external line outages. For illustration, consider matrices M (or Λ), where the number of rows represent the number of internal buses, and the number of columns indicates the number of external bus (this would be doubled in case of using Λ). Usually power networks in an interconnected system, are connected through a few buses (boundary

buses) with limited number of connections. Therefore, matrix B_{12} is a very sparse matrix. Figure 4, shows a schematic of a typical B_{12} for a given system after re-ordering rows and columns in B matrix in such a way that internal buses are in top followed by internal boundary buses.

Rows and columns of B_{12} correspond to the internal and external buses respectively. Therefore the shaded part in figure 4 represents part of B_{12} with nonzero entries (internal boundary buses), and the blank part, which corresponds to those internal buses with no direct connection to external buses, is a null matrix; Therefore, the equation set corresponding to the top part of B_{12} can be removed from the (13). It is interesting that even the shaded part of B_{12} is very sparse due to limited tie lines connecting internal buses to external system. This characteristic of B_{12} facilitates the process of solving the problem in the reasonable amount of time. As a result, the sparsity of M (and therefore Λ) is irrelevant of structure of B_{22}^{-1}. In other words, Λ in equation (13) is a sparse matrix with columns twice as many as number of external buses, and rows as many as number of internal boundary buses. Due to the limited number of internal boundary buses in an interconnected system, and due to the available error, solving equation (13) may not be possible without assist of a few real-time external measurements. In fact without application of PMUs, multiple solutions may cause the IP to find incorrect solution. Due to the fact that real-time synchronized data from selected external buses are available to internal power system dispatcher, and due to their direct connection with external buses, those external buses with PMUs can be treated as internal boundary buses, and therefore number of rows in Λ can be augmented by number of external buses with PMU. This will reduce the chance of getting multiple solutions through solving equation (13).

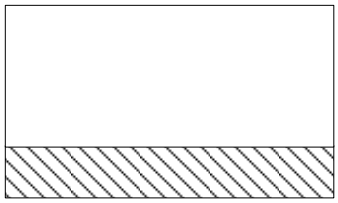

Figure 5. Typical B_{12} for a given system.

Equation (13) is a non-linear mixed integer problem, which can be solved using the proper IP package (i.e. GAMS [24]). Note that the IP problem in (13) minimizes the aggregated absolute value for error. Solving (13) identifies terminals of removed line in the external system. p identifies the pre-outage flow of the removed external line, and q represents the power loss between two ends of the external line outage due to being transferred from one end to another.

3. Simulation Results

3.1. Linear Formulation

Since the linear decoupled model, is an approximation to model the operation of power system, the proposed method should be checked for the error free system solution where power loss due to transfer from one end to another on a given line is zero. Once the method is validated using error free information, the method can be extended so that it works for the ac case as well.

In order to solve equation (13), information about pre-outage topology of entire system, as well as pre-outage and post-outage information of internal phase angles is required. To simulate the post outage internal phase angle, linear decoupled model of power system is used:

$$B\Delta\theta = \Delta P$$

$$\Rightarrow \quad \Delta\theta = B^{-1}\Delta P \qquad (14)$$

Line outage in external system will change the B matrix. Defining B' as the system post-outage B matrix, new state of the system $(\Delta\theta')$ can be calculated as follows:

$$\Delta\theta' = (B')^{-1}\Delta P \qquad (15)$$

The objective is to obtain a new set of power injection so that imposing them to the pre-outage system topology yields same states as the one calculated in (15). This can be accomplished as follows:

$$\Delta P_1 = B\Delta\theta' \qquad (16)$$

Where ΔP_1 represents a new set of injections required to obtain $\Delta\theta'$ when pre-outage topology is in play. Since the operator has no knowledge of real-time external data, both $\Delta\theta'$, and ΔP_1 can be divided into two sub-matrices: the part corresponding to the internal system is followed by the part corresponding to the external system this can be formulated as follows:

$$P_1 = \begin{bmatrix} P_{1-Internal} \\ \\ P_{1-External} \end{bmatrix} \quad , \theta' = \begin{bmatrix} \theta'_{Internal} \\ \\ \theta'_{External} \end{bmatrix} \qquad (17)$$

Thus $\Delta\theta_1$, and ΔP_1 in (8) are defined as follows:

$$\Delta\theta_1 = \theta'_{Internal} - \theta_{internal-BC}$$
$$\Delta P_1 = P_{1-Internal} - P_{1-Internal-BC} \qquad (18)$$

Where $\theta_{internal-BC}$, and $P_{1-Internal-BC}$ are base case values of the internal, phase angles and active power injections respectively.

To validate the method, IEEE 118 bus system [23] is used as a test bed. First the system is divided into two parts to simulate the internal and external system, and then different external line outages are imposed to the system to test the validity of the method.

Let assume that internal system is constituted of buses 1 through 45, 113,114,115, and 117. And external system includes buses 46 through 112, 116, and 118. Schematic of the two sub-systems and their connections is shown in figure 3.

To test the accuracy of the proposed method, different line outages are imposed to the external system, the outcome is calculated based on (14)-(18).

The updated data used as the post outage information in this section is error free since it is calculated using equations (14)-(18), therefore the error term in (7) needs to be dropped and the simpler formulation should be used to solve the problem (12). Then an IP package [24] is used to solve this equation.

Although it is critical for internal power system operator to be notified of major external line outages, due to their significant impact on internal security analysis, the method is capable of identifying both major and minor external line outages due to lack of error in this part of study. Results are shown in table 1.

Table.1. Test result for 118 bus system

Line outage	P (Pre-outage flow on removed line)	Solution found for X	
		-1 at bus	+1 at bus
59-63	7.608	59	63
77-80	3.003	77	80
60-61	6.810	60	61
68-116	0.948	116	68
96-82	0.332	82	96
100-101	0.532	100	101
103-104	0.562	104	103
80-98	1.631	98	80

The first four rows in table 1, correspond to major lines in external line outage, following rows correspond to external minor line. Although unreported minor external line outage does not have a significant impact on security analysis, being able to identify minor lines can increase the reliability of the proposed method.

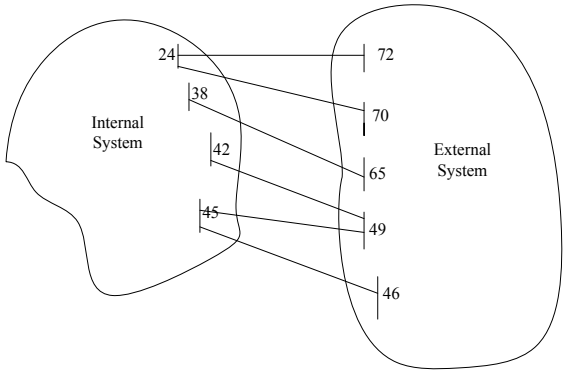

Figure 6. Internal and external system boundaries in IEEE 118 bus system

Next, the proposed method will be tested for the case that both operating change and topology change happen between two scans. Contrary with the previous case, errors are introduced to the system since the proposed method treat any change in operation condition as additional error. While ΔP_2 has only two non-zero entries in case of single line outage with constant operating condition between two scans, for a system with *M* external buses, ΔP_2 is a full vector with two large entries and *(M-2)* small entries in case of change of topology and operating conditions between two scans. Small entries created due to load change in the system and two large entries corresponding to terminals of the removed line. The small entries in ΔP_2 can be treated as errors; therefore, (12) should be used to solve the problem of this type. Table 2, shows the solution of the IP problem for

the outage of three major line in the external system, using the DC power flow solution in case of change of both topology and operating condition between two data selections. Note that the assumption is to run the test so frequently that the change of operating conditions will be limited at a certain threshold (2% of the base case loading). The lower the change in operating conditions, the higher the chance of identifying the terminals of the removed line correctly. Obviously in case of having larger change in operating condition the proposed method is facing the chance of getting multiple solutions and this can be restored with the help of real-time data from the external system.

Table 2. Results for 118 bus system with 2% change in load/generation

Line outage	P (Pre-outage flow on removed line)	ρ	Solution found for X	
			-1 at bus	+1 at bus
77-80	3.742	0.084	77	80
59-63	6.285	0.068	59	63
60-61	7.285	0.073	60	61

3.2. Nonlinear Formulation

The objective of this part of report is to validate the method when actual ac power flow solution is used. The proposed method is tested using two different scenarios. The first scenario is the case where the external operating condition remains approximately constant between two measurement scans before and after the line outage. In case the operating condition changes between two scans, these changes in load/generation will be treated as extra errors. It is critical to emphasize the importance of having external system PMU measurements in identifying the external line outages. While fault status of minor external lines does not have a notable impact on internal security analysis, wrong status of major external lines may cause serious consequences in security analysis, therefore identification of major external line outages is of interest of most of utility companies. This can be done by using the real-time data for all internal buses and data from those external buses whose real-time data available through PMUs.

The IEEE 30 bus system is used as a test bed to validate the proposed method. It is assumed that test is executed frequently enough to ensure that the changes in operating conditions remain below a certain threshold (2% of base case loading). IEEE 30 bus system is first split down into two sub-systems representing the internal and external

systems. It is assumed that the internal system is composed of buses 23 through 30, and the external system contains buses 1 through 22. Figure 1 shows the schematic description of the internal and external systems.

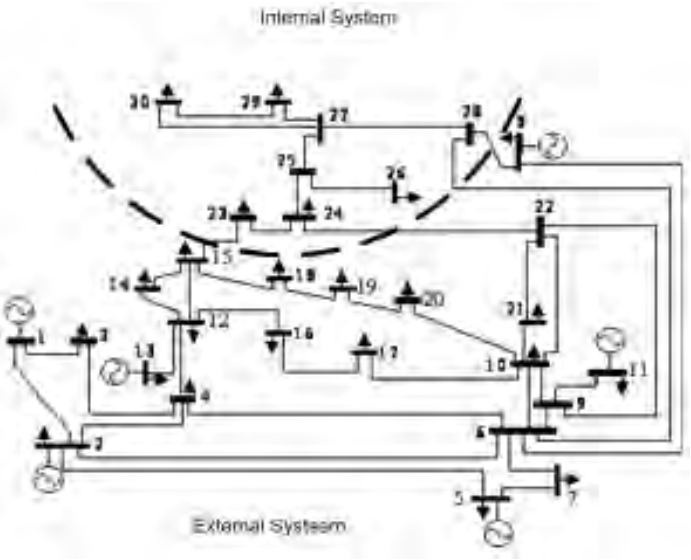

Figure 7. IEEE 30 bus system split into two sub-systems

The same system described in section 3.1 A, is used to validate the method for the ac case. Table 2 shows the test results for four different line outages in external system. Assist of PMUs are required to solve the problem in this part of study. Although high number (14 external PMUs) of PMUs is required to identify the minor external line outages, lower number of PMUs (8 PMUs) can handle accurate identification of major line outages in external system. Location of external PMUs in IEEE 118 bus system is chosen based on the method described in [25].

Table 3, shows the results of external line outage identification, using the proposed method. Note that this part of study is done based on the assumption of constant operating condition of external system between two scans. The first three rows in table 3 represent the major line outage in external system, and the last one shows a minor line outage identified using the proposed method.

Table.3. Test result for IEEE 30 Bus system, line outage with constant operating condition

Line Outage	P	Solution for X		q	J
		+1 @ bus	-1 @bus		
2-6	1.050	2	6	0.052@2	0.044
12-4	1.103	4	12	-0.055@12	0.036
3-4	7.382	3	4	0.426@3	0.028

Table 4. Test results for 118 bus system using AC power flow solutions

Line outage	P	Solution found for A		q	J
		+1@ bus	-1@ bus		
77-80	3.477	80	77	-0.056 @ 77	0.081
59-63	5.100	59	63	-0.2248 @ 59	0.197
60-61	7.216	61	60	0.012 @61	0.087
94-95	1.389	94	95	0.024 @94	0.12

While it is important to be able of identifying the line outage when the operating condition remains constant between two samples, the more complicated, and more realistic case is the case where both load, and topology change happens between two samples.

Table 5 and 6, shows the result for the case where both topology and operation condition of the system change between two snap shots. It is assumed that the package is executed so often that operating condition of the system does not change more than 2% between two steps. Results shown in table 5 and 6 are obtained for the case that loads/ generations in post outage system is increased by 2%. In case that the internal system operator wishes to run the test less frequently, the probability of having changes in system operating conditions in excess of 2% will be higher and this may necessitate the use of a higher number of external PMUs in order for the method to identify the correct line outage.

The only remaining condition which is not discussed so far in this report is the case of constant topology with dynamic operating condition between two consecutive scans. In the case of operating condition change with constant topology, no feasible solution can be found for equation (13) due to the last constraint in (13). As mentioned, presence of last constraint in (13) forces the solver to find two non-zero entries (corresponding to the terminals of the removed line) whose absolute value is larger than other entries of ΔP_2. Small entries in ΔP_2 are considered as entries in *e* vector. In case of load/generation

change with constant topology, ΔP_2 is a full vector whose entries are all small due to load/generation change in entire external system. These small entries are created due to the approximation error and/or the change in load/generation. Integer programming solution as defined in equation (13), will be looking for two large entries (line outage terminals) along with a vector of small entries (error). Therefore, in case of change in operating condition with no topology change, the optimal solution cannot be found with a pair of large entries in ΔP_2, and thus, the optimization will return a no feasible solution warning for the problem (13).

Table.5. Test result for IEEE 30 Bus system, line outage with 2% change in operating condition

Line Outage	P	Solution for X		q	J
		+1 @ bus	-1 @bus		
2-6	0.979	2	6	-0.049@6	0.032
12-4	1.126	4	12	-0.056@12	0.010
3-4	8.732	3	4	0.362@3	0.039

Table 6. Test result for IEEE 118 Bus system, line outage with 2% change in operating condition

Line outage	P	Solution found for A		q	J
		+1@ bus	-1@ bus		
77-80	3.766	80	77	0.036 @ 80	0.398
59-63	5.653	63	59	-0.171 @ 59	0.317
60-61	7.195	61	60	0.009 @61	0.08

4. Conclusions

This report describes the results of an investigation whose objective is to develop a method of tracking topology changes in the external system. Specifically, the report considers transmission line outages as the sources of topology changes and formulates the problem accordingly.

Initial formulation makes use of the linear decoupled power flow model and develops a solution for this simplified formulation. This is then extended to the full AC case where non-linear measurement equations are used. An optimization problem is solved in order to determine the line that is switched in the external system.

IEEE 30 and 118 bus test systems are used to illustrate the performance of the proposed method. The method can be applied to actual utility systems provided that internal and external system models are available along with internal system measurements and any existing PMU measurements from the external system.

References

[1] A. Bose, and K. Clements, 'Real-time modeling of power networks', *Proc. IEEE,* Dec. 1987, pp. 1607-1622

[2] F.F. Wu, 'Power system state estimation: a survey', *Electric Power and Energy Systems,* 1990, 12, (2), pp. 80-87

[3] H.-J. Koglin, T.H. Neisius, G. Beiβler, and K.D. Schmitt, 'Bad data detection and identification', *International Journal of Electric Power and Energy Systems, April* 1990, 12, (2). pp. 94-103.

[4] T.E. DyLiacco, 'The role and implementation of state estimation in an energy management system', *International Journal of Electric Power and Energy Systems,* 1990, vol. 12, no.2 , pp. 75-79.

[5] P. Bonanomi and G. Gramberg, 'Power system data validation and state calculation by network search techniques', *IEEE Trans. on* PAS-102, 1983, pp. 238-249.

[6] R.L. Lugtu, D.F. Hackett, K.C. Liu, and D.D. Might, 'Power system state estimation, detection of topological errors', *IEEE Trans. on* PAS-99, 1980, pp. 2406-2412.

[7] C.N. Lu, J.H. Teng, and B.S. Chang, 'Power system network topology error detection', Proceeding of IEE, Generation, Transmission, and Distribution, Nov 1994, vol. 141, issue 6, pp.623-629.

[8] K.A. Clements and P.W. Davis, 'Detection and identification of topological errors in electric power systems', *IEEE* Trans. on Power Systems, 1988, pp. 1748-1753.

[9] F.F. Wu, and W.H.E. Liu, 'Detection of topological errors by state estimation', *IEEE Trans. on Power Systems,* 1989, pp. 176-183.

[10] A. Simoes Costa and J.A. Leao, 'Identification of topology errors in power system state estimation', *IEEE Trans. on Power Systems, Nov.* 1993, vol. 8, no. 4, pp. 1531-1538.

[11] M.F. Allan, and A.M.H. Rashed, 'Power system topological error detection and identification', *International Journal of Electric Power and Energy Systems,* 1980, pp. 201-205.

[12] N. Singh and H. Glavitsch, 'Detection and identification of topological errors in online power system analysis', *IEEE Trans. on Power Systems,* 1991, pp. 324-331.

[13] N. Singh and F. Oesch, 'Practical experience with rule-based on-line topology error detection'. Proceedings of 1993 IEEE Conference on *Power Industry Computer Applications,* Scottsdale, Arizona, 1993, pp. 306-312.

[14] F.L. Alvarado, 'Determination of external system topology errors' *IEEE Trans. on* PAS-100, No.11, pp. 4553-4561, 1981.

[15] J.E. Tate, and T.J. Overbye, 'Line outage detection using phasor angle measurements' , *IEEE Trans. on Power Systems,* vol.23, no. 4, Nov 2008, pp 1644-1652.

[16] US-Canada Power System Outage Task Force, Final Report on August14, 2003 the Blackout in the United States and Canada, 2004. [Online].

[17] E. Lourenço, A. Costa, K. Clements, and R. Cernev, 'A topology error identification method directly based on collinearity tests,' *IEEE Trans. on Power Systems*, vol. 21, no. 4, pp. 1920–1929, Nov. 2006.

[18] A. Abur, H. Kim, and M. Çelik, 'Identifying the unknown circuit breaker statuses in power networks,' *IEEE Trans. on Power Systems*, vol. 10, no. 4, pp. 2029–2037, Nov. 1995.

[19] US-Canada power system outage task force, final report on the August 14 2003 blackout in the United States and Canada.

[20] "Steps to establish a real-time transmission monitoring system for transmission owners and operators within the eastern and western interconnections," U.S. Department of Energy and federal energy regulatory commission, Feb. 2006.

[21] R.Lee, H.Cai, A.Beard, J.Scott, "ICCP implementation for distributed control system"

[22] O. Alsac, B. Stott, W.F. Tinney, "Sparsity-Oriented compensation methods for modified network solutions" IEEE Transaction on Power Apparatus and Systems, Vol. PAS-102, No. 5, May 1983, pp1050-1060.

[23] Power system test case archive, available at http://www.ee.washington.edu/research/pstca/.

[24] 'GAMS- A User's Guide' tutorial by R.E.Rosenthal ,GAMS development Corp. 2008. Available online at : http://www.gams.com/dd/docs/bigdocs/GAMSUsersGuide.pdf

[25] R.Emami, A. Abur, "Robust measurement design by placing synchronized phasor measurements on network branches" IEEE Transaction on Power Systems, Vol. 25, No. 1, Feb. 2010, pp 38-43.